

ANALYTIC CALCULATIONS OF CERTAIN
SCATTERING PARAMETERS FROM
MODE CONVERSION EQUATIONS

Chung-Sang Ng

Certificate of Approval:

Joseph D. Perez
Professor, Physics

D. Gary Swanson, Chairman
Professor, Physics

James D. Hanson
Associate Professor, Physics

Richard A. Zalik
Professor, Mathematics

Norman J. Doorenbos, Dean
Graduate School

Style manual or journal used Physical Review Style and Notation Guide,
First Edition, 1983

Computer software used L^AT_EX

ANALYTIC CALCULATIONS OF CERTAIN
SCATTERING PARAMETERS FROM
MODE CONVERSION EQUATIONS

Chung-Sang Ng

A Dissertation
Submitted to
the Graduate Faculty of
Auburn University
in Partial Fulfillment of the
Requirements for the
Degree of
Doctor of Philosophy

Auburn, Alabama

June 8, 1994

VITA

Chung-Sang Ng, son of Man Sing Ng and Yuet Ho Mok, was born on August 23, 1962, in Hong Kong. He attended Ho Man Tin Government Middle School, graduated in 1981, and then entered The Chinese University of Hong Kong in the same year. During his undergraduate study, he was elected as the president of the Student Union of The Chinese University of Hong Kong of 1984. He received the degree of Bachelor of Science (Physics) in July, 1986. Immediately after that, he entered the Graduate School of The Chinese University of Hong Kong, and received the degree of Master of Philosophy (Physics) in July, 1988. After graduation, he worked for the Physics Department of The Chinese University of Hong Kong as a full time Teaching Assistant for one year. He entered the Graduate School of Auburn University in September, 1989, and entered the Doctor of Philosophy program of the Physics Department in October, 1990. He married Wan-Ju Tsai, daughter of Cheng-Chi Tsai and Pi-Chiao Huang, on August 25, 1990.

DISSERTATION ABSTRACT

ANALYTIC CALCULATIONS OF CERTAIN
SCATTERING PARAMETERS FROM
MODE CONVERSION EQUATIONS

Chung-Sang Ng

Doctor of Philosophy, June 8, 1994
(M. Phil. , The Chinese University of Hong Kong, 1988)
(B. S. , The Chinese University of Hong Kong, 1986)

94 Typed Pages

Directed by D. Gary Swanson

An analytical method is developed to calculate some scattering parameters from mode conversion equations which models the wave propagation in weakly inhomogeneous media near a back-to-back resonance-cutoff pair. The result is an analytic series expression. This method is applied to calculate the nonzero fast wave reflection coefficient from a fourth order equation which can model cases such as second ion cyclotron harmonic, second electron cyclotron harmonic, and some other situations. Numerical values from this series are compared to those calculated by the conventional method, namely, solving an integral equation iteratively. They agree with each other very well whenever both the series and the iteration converge. This result is based on a new method of evaluating integrals derived from the integral equation without having to solve the equation itself. Some empirical formulas based on the conventional method are shown to be good approximations but not

exact identities. We also calculate the nonzero reflection coefficient for a sixth order equation which models cases like the third ion or electron harmonic. The general characteristic for this reflection coefficient is very similar to that of the fourth order equation and the convergence properties of the series of both cases are also very similar. The proof shows that some scattering parameters are independent of absorption in the fourth order equation, which represents coupling between three wave branches, is extended to a sixth order equation, which represents coupling between five wave branches. The previous proof was done by considering contours in the u -plane, but this extended proof is in the k -plane, where $k = i \tan u$, because the u -plane is not convenient in this five branch problem. The analytic method is applied to this sixth order equation to calculate a nonzero mode conversion coefficient between the two fast wave branches that have different wavelengths but propagate in the same direction, and the reflection coefficient for the fast wave with the longer wavelength. Empirical formulas are found for these two coefficients. It is shown that this mode conversion coefficient is not exactly independent of absorption. However, it is found that the dependence is weak if the ratio of the wavelengths of the two type of fast waves does not differ greatly from unity. This explains a previous numerical result showing that this coefficient was independent of absorption to the numerical accuracy. The series found by this method does not always converge numerically. In some cases, this is because of the limited numerical accuracy of the computer, but in some other cases, the divergence seems intrinsic. The study of the convergence properties of this kind of series, or attempts to sum it analytically, should be a challenging and interesting research topic in the future.

ACKNOWLEDGMENTS

I would like to thank Dr. Gary Swanson for his advice and support. Thanks to Dr. Joseph Perez, Dr. James Hanson, and Dr. Richard Zalik for being my advisory committee members. I appreciate Dr. Jianlong Hu and Dr. Vadim Shvets for helpful discussions. Finally, thanks to my wife Wan-Ju Tsai for her patience and encouragement.

TABLE OF CONTENTS

I	INTRODUCTION	1
II	THREE BRANCH PROBLEM	12
	<u>Fourth Order Equation</u>	12
	Integral equation	12
	Integration	15
	Comparisons	21
	<u>Sixth Order Equation</u>	27
	<u>Discussion</u>	33
III	FIVE BRANCH PROBLEM	35
	<u>Integral Equations</u>	35
	<u>Solutions for Complex z</u>	48
	<u>Scattering Parameters</u>	57
	Independence of Absorption	57
	Series Method	58
	<u>Discussion</u>	71
IV	CONCLUSION	73

LIST OF TABLES

2.1	Case (i) with large λ^2 , $n_e = 5 \times 10^{19} \text{ m}^{-3}$, $L = 1 \text{ m}$, $B = 6 \text{ T}$, $T_i = 1000 \text{ eV}$	22
2.2	Case (i) with $\lambda^2 \sim 3$, $n_e = 1 \times 10^{20} \text{ m}^{-3}$, $L = 2 \text{ m}$, $B = 3 \text{ T}$, $T_i = 1000 \text{ eV}$	22
2.3	Case (i) with $\lambda^2 \sim 0.6$, $n_e = 2 \times 10^{20} \text{ m}^{-3}$, $L = 3 \text{ m}$, $B = 3 \text{ T}$, $T_i = 1000 \text{ eV}$	23
2.4	Case (ii) with $X = 0.114$, $n_e = 4 \times 10^{19} \text{ m}^{-3}$, $L = 0.15 \text{ m}$, $B = 3 \text{ T}$. .	24
2.5	Case (ii) with $X = 0.2057$, $n_e = 5 \times 10^{19} \text{ m}^{-3}$, $L = 2 \text{ m}$, $B = 2.5 \text{ T}$. .	24
2.6	Case (ii) with $X = 0.28575$, $n_e = 1 \times 10^{20} \text{ m}^{-3}$, $L = 0.2 \text{ m}$, $B = 3 \text{ T}$. .	24
2.7	Case (ii) with $X = 0.45725$, $n_e = 1.6 \times 10^{20} \text{ m}^{-3}$, $L = 0.2 \text{ m}$, $B = 3 \text{ T}$. .	25
2.8	Comparison of results calculated from Eq. (2.20) and Eq. (2.23) up to 195 terms with $\lambda^2 = 200$, $\alpha = 0.01$ and $z_0 = -\gamma/\lambda^2$. For P_2 and q_2 , $\gamma = 3$; for P_{3a} and q_{3a} , $\epsilon = 1$, $\gamma = 3$; for P_{3b} , $\epsilon = 0.1$, $\gamma = 3.9$; for P_{3c} , $\epsilon = 3.9$, $\gamma = 0.1$	29
2.9	Comparison of results calculated from Eq. (2.20) and Eq. (2.23) up to 195 terms with $\lambda^2 = 20$, $\alpha = 0.2$ and $z_0 = -\gamma/\lambda^2$. For P_2 and q_2 , $\gamma = 7$; for P_{3a} and q_{3a} , $\epsilon = 1$, $\gamma = 7$; for P_{3b} , $\epsilon = 0.1$, $\gamma = 7.9$; for P_{3c} , $\epsilon = 7.9$, $\gamma = 0.1$	30

2.10	Comparison of results calculated from Eq. (2.20) and Eq. (2.23) up to 195 terms with $\lambda^2 = 3$, $\alpha = 0.6$ and $z_0 = -\gamma/\lambda^2$. For P_2 and q_2 , $\gamma = 2.6$; for P_{3a} and q_{3a} , $\epsilon = 1$, $\gamma = 2.6$; for P_{3b} , $\epsilon = 0.1$, $\gamma = 3.5$; for P_{3c} , $\epsilon = 3.5$, $\gamma = 0.1$	31
3.1	Nonrelativistic case with $\lambda^2 = 20$, $ \alpha_2 = 0.12$, $ \alpha_4 = 0.001$ and $\kappa = 2$. Note that $P_0 = 0.3317\%$	65
3.2	Nonrelativistic case with $\lambda^2 = 200$, $ \alpha_2 = 0.12$, $ \alpha_4 = 0.001$ and $k_0 = 0.5$. Note that $P_0 = 0.3317\%$	65
3.3	Relativistic case with $\lambda^2 = 100$, $ \alpha_2 = 0.12$, $ \alpha_4 = 0.001$ and $\kappa = 0.6$. Note that $P_0 = 0.3317\%$	68
3.4	Relativistic case with $\lambda^2 = 100$, $ \alpha_2 = 0.12$, $ \alpha_4 = 0.001$, $k_0 = 0.9$ and $n = 119$. Note that $P_0 = 0.3317\%$	68

LIST OF FIGURES

2.1	Integration contours of I_{22} for the $\gamma > -1$ case.	17
2.2	Integration contours of I_{22} for the $\gamma < -1$ case.	17
2.3	Plot of $1 - q_a$ and $1 - q_n$ verse κ , where q_a and q_n are the values in Table 2.3	23
2.4	Plot of $7 - q_a$ and $7 - q_n$ verse κ , where q_a and q_n are the values in Table 2.4.	25
3.1	Schematic plot of the dispersion relation for the + case.	38
3.2	Schematic plot of the dispersion relation for the - case.	39
3.3	General contours of f_j 's for the + case.	40
3.4	General contours of f_j 's for the - case.	41
3.5	Topology of the contours for $z \rightarrow \infty \exp(i\theta)$ with $0 \leq \theta < \theta_1$, plotted for $\theta = 0$	42
3.6	Topology of the contours for $z \rightarrow \infty \exp(i\theta)$ with $\theta_1 < \theta < \theta_2$, plotted for $\theta = \pi/3$	43
3.7	Topology of the contours for $z \rightarrow \infty \exp(i\theta)$ with $\theta_2 < \theta < \theta_3$	44
3.8	Topology of the contours for $z \rightarrow \infty \exp(i\theta)$ with $\theta_3 < \theta < \theta_4$, plotted for $\theta = 2\pi/3$	45
3.9	Topology of the contours for $z \rightarrow \infty \exp(i\theta)$ with $\theta_4 < \theta \leq \pi$, plotted for $\theta = \pi$	46

3.10	Integration contours on the complex plane for some of the $I_{jk}^{\pm}(z)$ of fast waves for the $-$ case.	53
3.11	Integration contours on the complex plane of $I_{7k}^{+}(z)$ for $k = 1, 2, 3, 4$ of the $-$ case.	54

ANALYTIC CALCULATIONS OF CERTAIN
SCATTERING PARAMETERS FROM MODE
CONVERSION EQUATIONS

CHAPTER 1

I. INTRODUCTION

Effects like transmission, reflection, mode conversion and absorption usually exist when a wave propagates in a weakly inhomogeneous medium through a back-to-back resonance-cutoff region which occurs at harmonics of the cyclotron frequencies in a hot magnetized plasma. These phenomena can be modeled by different kinds of high order one dimensional ordinary differential equations (called mode conversion equations here). One of the simplest kinds of these is a fourth order equation of the form[1, 2, 3, 4]

$$f^{iv} + \lambda^2 z(f'' + f) + \gamma f = 0 , \quad (1.1)$$

where λ and γ are real constants. This is the mode conversion equation without absorption. Adding the absorption, the equation becomes[5, 6, 7]

$$\psi^{iv} + \lambda^2 z(\psi'' + \psi) + \gamma\psi = h(z)(\psi'' + \psi) , \quad (1.2)$$

where $h(z)$ is the absorption function which generally must fall off at least as fast as z^{-1} as $|z| \rightarrow \infty$. For $|z| \rightarrow \infty$, i.e. the asymptotic region, this equation reduces to Eq. (1.1). This equation can model many different physical situations which involve a resonance. We will explicitly consider two of them later: (i) second ion cyclotron harmonic with $\gamma > -1$; (ii) second electron cyclotron harmonic with $\gamma < -1$. Some other physical situations such as the two ion hybrid[7] and electron O-mode fundamental[4] can also be modeled by this equation.

Let us discuss the reason why mode conversion effects are so important in considering wave propagation in an inhomogeneous plasma. The first step to treat a wave propagation problem is to consider a wave in a uniform medium, such as a cold magnetized plasma. The dispersion relation that the wave has to satisfy in order to propagate in the medium can be derived by the Maxwell Equation, making use of the dielectric tensor of the medium, see, e.g., [4]. This dispersion relation can be expressed as a phase velocity surface or a wave vector surface for a given frequency. It is well known that the topology of these surfaces for a cold plasma can be classified into regions in the CMA diagram which depends on only two plasma parameters, the density and the magnetic field strength. That is, the topology of the wave vector surface is the same inside each region, but will change across the boundary of that region. What happens on the boundaries is that there is either a cutoff (with refractive index being zero), or a resonance (with refractive index being infinite).

Back to the problem of an inhomogeneous plasma, the density and magnetic field strength are now functions of position (consider a steady state situation). A wave propagating in an inhomogeneous plasma will generally cross the boundaries of the CMA diagram, passing through a cutoff or a resonance. However, a true resonance is not allowed in a realistic physical process. There have to be some mechanisms to resolve these resonances, for example, by warm plasma effects. It has been demonstrated by Stix[8] that some resonances will be resolved to a back-to-back resonance-cutoff pair and that some wave energy will be converted into a warm plasma wave. Swanson has also shown that linear mode conversion is always involved to some extent in resolving every plasma resonance in an inhomogeneous

plasma[7, 4]. It is also found that mode conversion can happen in a warm plasma where there is no corresponding resonance in a cold plasma, e.g., when the wave frequency is close to the harmonics (not including the fundamental) of ion or electron cyclotron frequency. So we see that the mode conversion process is present in most situations of wave propagation in an inhomogeneous plasma. Because of this, the mode conversion effects have been applied for heating or diagnosis of fusion plasmas[9]–[16], since most laboratory plasmas are inhomogeneous. Determinations of the scattering parameters (transmission, reflection and mode conversion coefficients) are very important for these applications.

One possible way to describe mode conversion effects and to calculate the scattering parameters is to model the physics by mode conversion equations mentioned above. The basic steps to derive these model equations is by first considering a warm plasma with an inhomogeneity in one dimension only and require the inhomogeneity to be weak enough such that it can be approximated by constant and linear terms. For example, the mode conversion equations we discuss in this dissertation are derived by considering a linear inhomogeneity of the magnetic field strength in a direction perpendicular to the direction of the magnetic field itself. The warm plasma dispersion relation, which now depends on spatial position, is then used and its series expansion in the Larmor radius is truncated by using a small Larmor radius approximation. Finally, the component of the wave vector along the direction of the inhomogeneity is converted to a differential operator. A high order one dimensional ordinary differential equation to model the mode conversion effect can thus be obtained. Historically, such model equations started with simpler forms. A

second order equation called the Budden equation,

$$z(f'' + f) + 2\eta f/\pi = 0 ,$$

which models a cold plasma back-to-back pole and zero pair, was first analyzed by Budden[17] with the transmission and reflection coefficients obtained analytically,

$$T^2 = e^{-2\eta} , \quad R^2 = (1 - T^2)^2 \text{ or } 0 .$$

However, since $T^2 + R^2 < 1$, the energy is not conserved. Moreover, it cannot describe the conversion to a warm plasma wave. Another equation studied earlier is the fourth order equation

$$f^{iv} + \lambda^2(zf'' + \alpha f' + \beta f) = 0 .$$

This equation was studied by Wasow[18] with $\alpha = 0$, and later by Rabenstein[19] with $\alpha \neq 0$ and complex α, β . Based on their results, Stix[8] described the mode conversion between cold and warm plasma waves. He also discussed the necessity of the fourth order term in order to resolve the singularity[20]. A review of these early works was given by Golant and Piliya[21]. The $\gamma + 1 > 0$ case of Eq. (1.1) was analyzed independently by Erokhin[1] and by Ngan and Swanson[2]. The $\gamma + 1 < 0$ case was analyzed by Faulconer[22] and by Antonsen and Manheimer[23], using different methods. Up to here, the scattering parameters of these model equations can be obtained analytically. After including the effects of absorption, Eq. (1.1) becomes Eq. (1.2)[5, 6, 7]. The scattering parameters of this equation were first calculated numerically by an integral equation method[5].

It has been pointed out that odd order derivatives should be added to Eq. (1.1) and (1.2), with a much more complicated expression on the right hand side of

Eq. (1.2), in order to conserve energy[7]. However, from previous numerical results, the scattering parameters found by both sets of equations are close, especially for the reflection coefficient R_2 [7], so we will use the simpler equations for our analysis. We believe that the method we develop here should also work for the energy conserving equations, since the two sets of equations are very similar.

Analytic expressions for the scattering parameters, i. e., transmission, reflection and mode conversion coefficients, for Eq. (1.1) have long been known[4]. Solutions for Eq. (1.2), and thus scattering parameters, can be found by solving an integral equation iteratively, making use of the numerical solutions of Eq. (1.1) and of the adjoint equation of it[7] (note that Eq. (1.1) is not self-adjoint). Then the scattering parameters can be expressed by integrals I_{jk} with integrands being proportional to the product of $h(z)$ and solutions of the adjoint of Eq. (1.1) and Eq. (1.2) along the z -axis. Some empirical formulas have been found for these scattering parameters, e.g., $|R_2|^2 \approx R_{20}^2 \exp(-2\kappa^2)$ for the case (i) mentioned above, and $|R_2|^2 \approx R_{20}^2 \exp(-14\kappa^2)$ for case (ii), where $R_{20}^2 = [1 - \exp(-2\eta)]^2$, with $\eta = \pi(1 + \gamma)/2\lambda^2$. The parameter κ is a measure of the absorption strength. The dependence of κ on plasma parameters for the two physical cases will be presented in Chapter II.

Recently, by extending solutions of Eq. (1.1) and Eq. (1.2) into the complex z -plane, some of these integrals I_{jk} were shown to be zero identically by Swanson and Shvets[24]. Thus, fast wave transmission coefficients from both sides (which are equal to each other) and the fast wave reflection coefficient from the side which encounters the resonance before the cutoff (which is identically zero), were shown to be independent of absorption. However, analytic expressions for other scattering parameters which do change with absorption have been unknown so far. In this

research, we go further along this direction and develop a new method that may be used to calculate some of these nonzero integrals analytically[25]. This has been done successfully for the nonzero reflection coefficient R_2 for the above two cases (i) and (ii). The result is an analytic series expression. Numerical values from this series for these two cases are compared to those calculated by the conventional method, namely, solving an integral equation iteratively. They agree with each other very well whenever both the series and the iteration converge. The empirical formulas found from the numerical results of the integral equation method are shown to be good approximations but not exact identities. For cases with large λ^2 , small η and κ , the empirical formulas are very accurate as can be seen from summing the analytical series numerically, although these formulas also work relatively well outside this range of parameters.

We note that the above method is not the only approach used to solve the mode conversion problem. Other methods have been developed, including, e. g., direct numerical integration[6], finite element[26], finite difference[27], phase space method[28], and order reduction[29, 30, 31, 32]. Certain partial or approximate expressions of the scattering parameters have also been reported[31, 28, 32]. However, we will concentrate on the above integral equation method of solving Eq. (1.2) here. We emphasize that the analytical expression for the reflection coefficient given here is *exact* in the sense that no further approximation is used after we accept Eqs. (1.1) and (1.2), which are in a general mathematical form that may represent many other physical situations. In all other semianalytic methods, additional approximations are made before evaluating the reflection coefficient.

We also apply the method to calculate the nonzero reflection coefficient of a sixth order equation, which describes the third ion cyclotron harmonic[33],

$$\psi^{vi} + (1 - \epsilon)\psi^{iv} - \lambda^2 z(\psi'' + \psi) - \gamma\psi = h(z)(\psi'' + \psi) , \quad (1.3)$$

to see whether the method can apply to higher order equations. The results is very similar to that of the fourth order equation. They both give the same approximate empirical formula. The convergence properties of the series in both cases are also very similar. Both the fourth order equation and the sixth order equation describe coupling of three branches of propagating waves: two fast wave branches and a slow wave branch on the $z > 0$ side. We call these three branch problems.

An equation that describes coupling of five branches of propagating waves is[34]

$$\psi^{vi} + \lambda^2 z[\psi^{iv} + (1 + k_0^2)\psi'' + k_0^2\psi] + \gamma_2\psi'' + \gamma_0\psi = h(z)[\psi^{iv} + (1 + k_0^2)\psi'' + k_0^2\psi] , \quad (1.4)$$

where λ , γ_2 , γ_0 and k_0 are real constants. The parameter k_0 is the ratio of the wavelengths of the two fast wave branches as $|z| \rightarrow \infty$ and has been chosen to be always smaller than unity here. The dispersion relation for this equation is

$$-k^6 + \lambda^2 z[k^4 - (1 + k_0^2)k^2 + k_0^2] - \gamma_2 k^2 + \gamma_0 .$$

This relation is plotted on Figs. 3.1 and 3.2 for two cases, namely $\alpha_2, \alpha_4 > 0$ (+ case) and $\alpha_2, \alpha_4 < 0$ (− case), where

$$\begin{aligned} \alpha_2 &= (1 + \gamma_2 - \gamma_0)/2\lambda^2(1 - k_0^2) , \\ \alpha_4 &= (-k_0^6 - \gamma_2 k_0^2 + \gamma_0)/2\lambda^2 k_0(1 - k_0^2) . \end{aligned} \quad (1.5)$$

Eqs. (1.2) and (1.4) can both describe physical situations like second ion cyclotron harmonic and second electron cyclotron harmonic in an inhomogeneously

magnetized plasma. It is well known that only the X-mode exists along a direction perpendicular to the magnetic field if the wave frequency ω is smaller than the plasma frequency ω_p . So a five branch problem only exists for $\omega > \omega_p$ and it must be a five branch problem whenever the X-mode is propagating because the O-mode always exists for this case. However, Eq. (1.2) is frequently used to model the X-mode for all ω . This is because the coupling between X-mode and O-mode is usually weak (especially for small k_{\parallel} , the component of the wave vector along the direction of the magnetic field) and it is argued that we can treat the five branch problem as two separated three branch problems. Moreover, since it was found that all mode conversion coefficients of a three branch problem tend to zero as absorption increases, the coupling between the X-mode and the O-mode should become vanishingly small when the absorption is strong.

Note that in Figs. 3.1 and 3.2, whether the $k^2 = 1$ branch represents the X-mode (thus the $k^2 = k_0^2$ branch represents the O-mode) or the O-mode depends on the physical situation. In this dissertation, we call the $k^2 = 1$ branch u -mode and the $k^2 = k_0^2$ branch v -mode. For the second ion cyclotron harmonic and the second electron cyclotron harmonic with $4\omega_p^2/3 > \omega^2 > \omega_p^2$, $u = X$ and $v = O$. For the second electron cyclotron harmonic with $\omega^2 > 2\omega_p^2$, $u = O$ and $v = X$.

Another mode conversion equation that describes a five branch problem is an eighth order equation[34, 35, 36]

$$\begin{aligned} \psi^{viii} + \gamma_6 \psi^{vi} - \lambda^2 z [\psi^{iv} + (1 + k_0^2) \psi'' + k_0^2 \psi] - \gamma_2 \psi'' - \gamma_0 \psi \\ = h(z) [\psi^{iv} + (1 + k_0^2) \psi'' + k_0^2 \psi] , \end{aligned} \quad (1.6)$$

which can model physical situations like the third ion or electron cyclotron harmonic.

One surprising result from a previous study was that the nonzero mode conversion coefficient C_{23} from Eq. (1.6) between the X-mode and the O-mode branches propagating in the same direction appeared to be independent of absorption to the numerical accuracy[34, 36] (note that it is called C_{41} in Ref. [36]). If this result were true, then there is a great difficulty in understanding this by the separation scheme. The difficulty is that for large absorption, all mode conversion coefficients between fast and slow waves vanish for the two individual three branch problems and it is hard to imagine why the mode conversion coefficient between the two fast modes does not vanish after the two three branch problems are combined into a single five branch problem since the coupling is via an intermediate slow wave. Before we investigate further along this direction, it is better to calculate the same coefficient using other analytical methods to check this numerical result. We will present in detail the theory for Eq. (1.4) only, but will show that the results from both Eqs. (1.4) and (1.6) are very similar.

There is a standard method to calculate all scattering parameters from mode conversion equations like Eqs.(1.2), (1.4) or (1.6) analytically for $h = 0$ [37, 38]. For $h \neq 0$, there exists a well developed numerical method to calculate solutions and scattering parameters from these equations[5, 7, 36]. This method involves solving a “homogeneous equation” (i.e., with $h = 0$) by numerical contour integrations and then solving the “inhomogeneous equation” by converting it into an integral equation which is solved iteratively, using the solutions of the former equation to form the kernel. The scattering parameters can then be calculated by numerically integrating an integral involving h and solutions of these two equations.

We first extend the proof of Swanson and Shvets, showing that some fast wave scattering parameters from Eq. (1.2) are independent of absorption, to cover Eq. (1.4) to see if the coefficient C_{23} can also be shown to be independent of absorption. This extension turns out to be not quite straightforward. By this proof, many fast wave scattering parameters are shown to be independent of absorption. However, as we will see, the coefficient C_{23} is not one of them.

We then apply the analytical series method to calculate C_{23} . For completeness, we also try to apply it to calculate other nonzero fast wave scattering parameters. It turns out that this method only works for $C_{23}(C_{32})$ and R_4 which is the nonzero reflection coefficient for the fast wave with the longer wavelength. Empirical formulas are found for both coefficients. From these results, we find that C_{23} is not identically zero, but the dependence on absorption is usually much weaker than for other coefficients when k_0 is close to unity. We will also calculate C_{32} using the series method to see if it is equal to C_{23} as required by the reciprocity relations which have been proved analytically[39, 36].

In Chapter II, we will consider the three branch problem by first reviewing the integral equation method, and thus the integral expressions which arise in the scattering parameters. We then discuss the basic ideas of the series method and show explicitly how to calculate R_2 analytically for the ion and electron cases from Eq. (1.2). We will also compare results from this method to those calculated by the integral equation numerically. The results are also compared with those calculated from Eq. (1.3). In Chapter III, we will present the integral equations of Eq. (1.4) for both \pm cases for the five branch problem and show how to generalize solutions of the “homogeneous equation” for complex z values using contour integrations in the

complex k -plane. Also, we will be able to see why some scattering parameters are independent of absorption and why some scattering parameters can be calculated by the series method. Numerical results for C_{23} , R_4 and C_{32} will also be presented there. Conclusions will be given in Chapter IV. A simple example of the integration method used in this study will be given in the Appendix.

ANALYTIC CALCULATIONS OF CERTAIN
SCATTERING PARAMETERS FROM MODE
CONVERSION EQUATIONS

CHAPTER 2

II. THREE BRANCH PROBLEM

In this chapter, we describe how to apply a new method to calculate the nonzero fast wave reflection coefficient from mode conversion equations for three branch problems. The description for the fourth order equation (1.2) will be presented in detail. The results for the sixth order equation (1.3) will then be presented briefly to show that they are very similar to that of Eq. (1.2).

Fourth Order Equation

Integral equation

Eq. (1.1) can be solved exactly by using the method of Laplace[4]:

$$f_j(z) = c_j \int_{\Gamma_j} [\exp z g(k)] dk, \quad j = 1, 2, 3, 4, \quad (2.1)$$

where the Γ_j are contours in the complex k -plane which end at infinity with approach angles of $\pi/6$, $5\pi/6$, or $3\pi/2$, and

$$g(k) = -ik + \frac{i}{z} \left\{ \frac{k^3}{3\lambda^2} + \frac{k}{\lambda^2} + (i - \alpha) \ln(k + 1) + (i + \alpha) \ln(k - 1) \right\},$$

where $\alpha = (1 + \gamma)/2\lambda^2$. With a suitable choice of constants c_j , we can express the asymptotic behavior of f_j (note that the definitions in this dissertation are in

general different from those in previous papers on the subject[4]) as

$$\begin{pmatrix} 0 & T_1 & 0 & C_{14} \\ 1 & R_2 & 0 & C_{24} \\ 0 & C_{32} & 0 & C_{34} \\ 0 & C_{42} & 1 & R_4 \end{pmatrix} \begin{pmatrix} f_+ \\ f_- \\ \sigma_+ \\ \sigma_- \end{pmatrix} \xleftarrow{z \rightarrow \infty} \begin{pmatrix} f_1 \\ f_2 \\ f_3 \\ f_4 \end{pmatrix} \xrightarrow{z \rightarrow \infty} \begin{pmatrix} R_1 & 1 & C_{13} & 0 \\ T_2 & 0 & C_{23} & 0 \\ C_{31} & 0 & R_3 & 1 \\ C_{41} & 0 & C_{43} & 0 \end{pmatrix} \begin{pmatrix} f_+ \\ f_- \\ s_- \\ s_+ \end{pmatrix}, \quad (2.2)$$

for $\gamma > -1$, and

$$\begin{pmatrix} R_1 & 1 & 0 & C_{14} \\ T_2 & 0 & 0 & C_{24} \\ C_{31} & 0 & 0 & C_{34} \\ C_{41} & 0 & 1 & R_4 \end{pmatrix} \begin{pmatrix} f_- \\ f_+ \\ \sigma_+ \\ \sigma_- \end{pmatrix} \xleftarrow{z \rightarrow \infty} \begin{pmatrix} f_1 \\ f_2 \\ f_3 \\ f_4 \end{pmatrix} \xrightarrow{z \rightarrow \infty} \begin{pmatrix} 0 & T_1 & C_{13} & 0 \\ 1 & R_2 & C_{23} & 0 \\ 0 & C_{32} & R_3 & 1 \\ 0 & C_{42} & C_{43} & 0 \end{pmatrix} \begin{pmatrix} f_- \\ f_+ \\ s_+ \\ s_- \end{pmatrix}, \quad (2.3)$$

for $\gamma < -1$, with scattering parameters given by

$$S_{ij} = \begin{pmatrix} R_1 & T_1 & C_{13} & C_{14} \\ T_2 & R_2 & C_{23} & C_{24} \\ C_{31} & C_{32} & R_3 & C_{34} \\ C_{41} & C_{42} & C_{43} & R_4 \end{pmatrix} = S_{ij}^{(0)} = \begin{pmatrix} 0 & T & -C & 0 \\ T & C^2 & TC & C \\ -C & TC & T^2 & T \\ 0 & C & T & 1/2 \end{pmatrix}, \quad (2.4)$$

where $T = \exp(-\eta)$, $\eta = \pi|\alpha|$, $C^2 = 1 - T^2$, and

$$\begin{aligned} f_{\pm} &= \frac{-\pi e^{-\eta/2}}{C\alpha\Gamma(\pm i\alpha)} \exp \left\{ \pm i \left[\frac{-4}{3\lambda^2} + \alpha \ln 2 + z + \alpha \ln |z| \right] \right\}, \\ s_{\pm} &= \operatorname{sgn}(\alpha) \frac{\sqrt{\pi}}{\lambda^{3/2} z^{5/4}} \exp \left\{ \pm i \left[\frac{2}{3} \lambda z^{3/2} - \frac{z^{1/2}}{\lambda} - \pi/4 \right] \right\}, \\ \sigma_+ &= \frac{-i\sqrt{\pi} e^{-\pi\alpha}}{\lambda^{3/2} |z|^{5/4}} \exp \left\{ \frac{2}{3} \lambda |z|^{3/2} + \frac{|z|^{1/2}}{\lambda} \right\}, \\ \sigma_- &= -\operatorname{sgn}(\alpha) \frac{\sqrt{\pi} e^{\pi\alpha}}{\lambda^{3/2} |z|^{5/4}} \exp \left\{ -\frac{2}{3} \lambda |z|^{3/2} - \frac{|z|^{1/2}}{\lambda} \right\}. \end{aligned}$$

Only f_1, f_2, f_3 are physically allowed in an unbounded region. Using these we can find an integral equation that solves Eq. (1.2) [5, 7]:

$$\psi_k = f_k \mp \frac{1}{T} \begin{cases} f_2 I_{1k}^- + f_4 I_{0k}^- + f_1 I_{2k}^+ + f_0 I_{4k}^+, & \gamma > -1, \\ f_1 I_{2k}^- + f_5 I_{0k}^- + f_2 I_{1k}^+ + f_0 I_{5k}^+, & \gamma < -1, \end{cases} \quad (2.5)$$

where

$$I_{jk}^{\pm} = \frac{\pm 1}{2\pi i \lambda^2} \int_z^{\pm\infty} F_j(y) h(y) \Psi_k(y) dy ,$$

with

$$F_j = f_j'' + f_j , \quad \Psi_j = \psi_j'' + \psi_j , \quad (2.6)$$

and $f_0 \equiv f_3 - C f_1$, for $\gamma > -1$, $f_0 \equiv T(C f_2 + T f_3)$, $f_5 \equiv f_4 - C f_1/T$, for $\gamma < -1$. Eq. (2.5) can be solved iteratively using $\psi_k = f_k$ as the first trial function with f_k calculated numerically by Eq. (2.1). This can be done for the three physical solutions, $k = 1, 2, 3$, if $h(z)$ falls off at least as fast as z^{-1} as $|z| \rightarrow \infty$. For the $k = 4$ solution, this can be done only if $h(z)\sigma_+(z) \rightarrow 0$ fast enough as $z \rightarrow -\infty$. Numerically, this method converges in general, but may become divergent when the absorption is very large. After solving Eq. (2.5), scattering parameters can be found, making use of Eqs. (2.2)–(2.4), by

$$S_{jk} = S_{jk}^{(0)} \mp I_{jk} , \quad \text{for } \pm(\gamma + 1) > 0 ,$$

with

$$I_{jk} = \frac{1}{2\pi i \lambda^2} \int_{-\infty}^{\infty} F_j(z) h(z) \Psi_k(z) dz , \quad (2.7)$$

where we have already used the fact that $I_{jk} = I_{kj}$. In particular, the integral expression for R_2 is $R_2 = C^2 \mp I_{22}$. In the next section, we will show how to calculate this integral I_{22} analytically, without the need of solving Eq. (2.1) or Eq. (2.5) numerically.

Integration

To perform the integration of I_{22} , we must first specify the absorption function $h(z)$. For case (i), the second ion cyclotron harmonic with $\gamma > -1$,

$$h(z) = \lambda^2 \kappa [\zeta - 1/Z(-\zeta)] , \quad (2.8)$$

where the plasma dispersion function $Z(\zeta) = i\sqrt{\pi}w(\zeta)$, with w being the error function for complex argument[40]. The dependence of the dimensionless parameters on the plasma parameters are,

$$\begin{aligned} \lambda^2 &= 4(1/3 + p^2)V_A/n_{\perp}^3\omega\beta_i L , & \gamma &= -2(1/3 + p^2)/(1 + p^2) , \\ \zeta &= (z - z_0)/\kappa = -\omega x/k_{\parallel}v_i L , & \kappa &= n_{\perp}k_{\parallel}v_i L/V_A , \\ n_{\perp}^2 &= (1 + p^2)(1/3 - p^2)/(1/3 + p^2) , & p^2 &= (k_{\parallel}V_A/\omega)^2 , \\ z_0 &= -\gamma/\lambda^2 , & V_A &= \omega c/2\omega_{pi} , \\ \beta_i &= (v_i/V_A)^2 , & v_i^2 &= 2k_B T_i/m_i , & \omega_{pi} &= n_i q_i^2/m_i \epsilon_0 , \end{aligned}$$

where n_i is the ion density, q_i is the charge of the ion, m_i is the mass of the ion, k_B is the Boltzmann constant, T_i is the ion temperature, ω is the frequency of the propagating wave which is assumed to be much smaller than the plasma frequency, k_{\parallel} is the wavenumber of the wave along the direction of the magnetic field which is assumed to be perpendicular to the direction of its gradient, L is the characteristic length of the inhomogeneity of the magnetic field strength $B(x)$ so that $B(x) = B(1+x/L)$, with $B = m_i\omega/2q_i$. For case (ii), the second electron cyclotron harmonic with $\gamma < -1$,

$$h(z) = \lambda^2 \kappa \left[\zeta - 1/F_{\frac{7}{2}}(\zeta - 7/2) \right] , \quad (2.9)$$

with F_q being the relativistic plasma dispersion function [41, 42]. The dependence of the dimensionless parameters on the plasma parameters for this case are,

$$\begin{aligned}\lambda^2 &= 2\mu(1 - \alpha/3)c/n_\perp^3\omega\alpha L, & \gamma &= -2(1 - \alpha/6)/n_\perp^2, \\ \zeta &= (z - z_0)/\kappa = -\mu x/L, & \kappa &= n_\perp\omega L/\mu c, \\ n_\perp^2 &= (1 - \alpha/2)(1 - \alpha/6)/(1 - \alpha/3), & \alpha &= (2\omega_{pe}/\omega)^2, \\ z_0 &= -\gamma/\lambda^2, & \omega_{pe} &= n_e q_e^2/m_e \epsilon_0, & \mu &= m_e c^2/k_B T_e,\end{aligned}$$

where n_e is the electron density, q_e is the charge of the electron, m_e is the mass of the electron, T_e is the electron temperature, ω is now assumed to be larger than $\sqrt{2}\omega_{pe}$, k_\parallel is assumed to be zero, the magnetic field strength at $x = 0$ now is $B = m_e\omega/2q_e$. Note that the parameter κ is real and positive and is a measure of the strength of absorption. Note that both $Z(\zeta)$ and $F_q(\zeta)$ are analytic functions and have zeros only in the lower half ζ -plane. Also, solutions F_k and Ψ_k have been shown to be analytic everywhere[24]. Then, following Ref. [24], we can change the path of integration of I_{jk} , defined in Eq. (2.7), to the semicircles C_\pm : $z = R \exp(i\theta)$ with $R \rightarrow \infty$ and θ from $-\pi$ to 0 for case (i) (see Fig. 2.1), and θ from π to 0 for case (ii) (see Fig. 2.2).

In Ref. [24], solutions f_k and ψ_k have been extended to the complex z -plane, and it was shown that on these new contours C_\pm , both f_1 and $\psi_1 \propto \exp(\mp iz)$ and are thus exponentially small for both cases of $\pm(\gamma + 1) > 0$, and that f_2 and $\psi_2 \propto \exp(\pm iz)$ and are thus exponentially large. It was then concluded that $I_{11} = I_{12} = I_{21} = 0$, which means that $T_1 = T_2 = \exp(-\eta)$, and $R_1 = 0$, independent of absorption[24]. Our approach here to calculate I_{22} is to expand the integrand $F_2 h \Psi_2$ in an asymptotic series on C_\pm . Since $|z| \rightarrow \infty$ on the contour, all terms

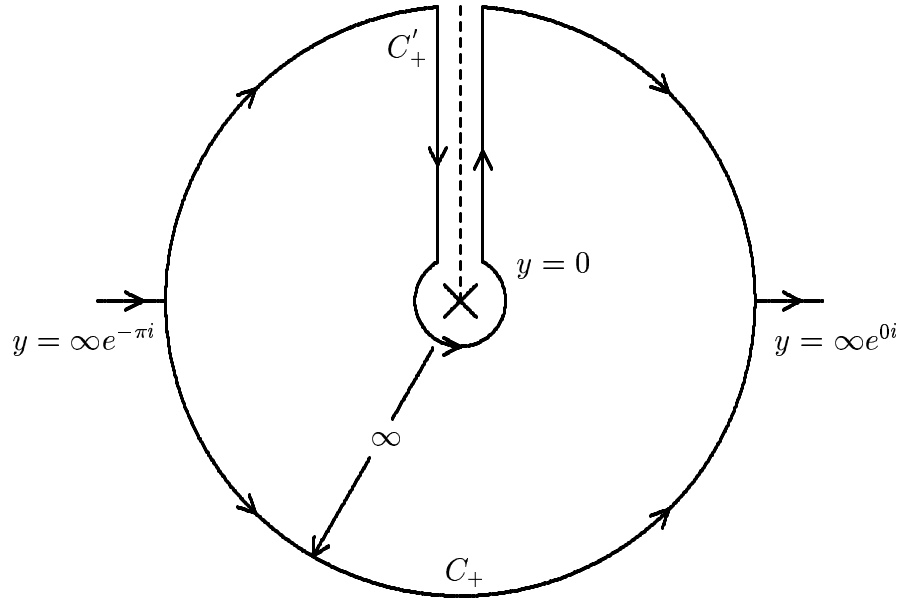


Figure 2.1: Integration contours of I_{22} for the $\gamma > -1$ case.

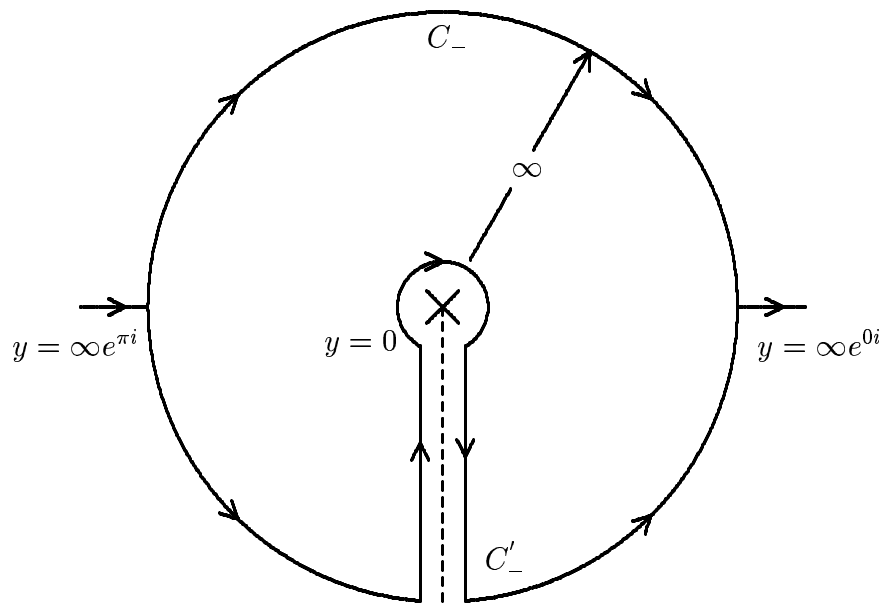


Figure 2.2: Integration contours of I_{22} for the $\gamma < -1$ case.

in this asymptotic series may be kept. Although the integrand is in general a divergent series in z^{-n} for any finite z , the series obtained after integration may become convergent for certain absorption functions $h(z)$. First of all, it is easy to expand $h(z)$ in asymptotic series,

$$h(z) \rightarrow \sum_{n=1}^{\infty} \frac{h_n^{\pm}}{y^n}, \quad \text{for } \pm(\gamma + 1) > 0, \quad (2.10)$$

where $y \equiv z - z_0$. This can be done by inverting the two asymptotic series,

$$Z(-\zeta) = \frac{1}{\zeta} \sum_{n=0}^{\infty} \frac{\Gamma(n + 1/2)}{\Gamma(1/2)\zeta^{2n}}, \quad (2.11)$$

and

$$F_q(\zeta) = \frac{1}{\zeta} \sum_{n=0}^{\infty} \frac{(-1)^n \Gamma(n + q)}{\Gamma(q)\zeta^n}, \quad (2.12)$$

on the path of integration C_{\pm} . First, we need to shift the argument of the $F_{\frac{7}{2}}$ function in Eq. (2.9) from $\zeta - 7/2$ to ζ . Let,

$$F_q(\zeta - q) = \sum_{n=1}^{\infty} \frac{A_n(q)}{\zeta^n}.$$

The coefficients $A_n(q)$ can be found, using Eq. (2.12), by

$$A_n(q) = -\frac{1}{\Gamma(q)} \sum_{m=1}^n (-1)^m \Gamma(q + m - 1) C_{n-1}^{n-m} q^{n-m},$$

where the $C_n^m = n!/m!(n-m)!$ are the binomial coefficients. The first few values of A_n are $A_1 = 1, A_2 = 0, A_3 = q$. Then we can invert F_q by,

$$\frac{1}{F_q(\zeta - q)} = \zeta \left[1 + \sum_{n=2}^{\infty} \frac{C_n(q)}{\zeta^n} \right], \quad (2.13)$$

where

$$C_{2m+\frac{1}{2}\pm\frac{1}{2}}(q) = \sum_{n=1}^m [-A_3(q)]^n D_{2(m-n)+\frac{1}{2}\pm\frac{1}{2}}(q, n),$$

$$\begin{aligned}
D_n(q, m) &= \sum_{k=0}^n D_{n-k}(q, m-1) D_k(q, 1) , \\
D_n(q, 1) &= A_{n+3}(q)/A_3(q) .
\end{aligned}$$

Finally we can get the coefficients h_n^- of Eq. (2.10) by ,

$$h_n^- = -\lambda^2 \kappa^{n+1} C_{n+1}(7/2) . \quad (2.14)$$

We can also invert the asymptotic series of $Z(-\zeta)$ of Eq. (2.11), using calculations similar to Eqs. (2.13)–(2.14), to get h_n^+ .

To find the asymptotic series for f_2 and ψ_2 , we first note that only the part of them with leading behavior $\exp \pm i(y + \alpha \ln y)$ on C_\pm contribute to the integral I_{22} , so

$$2\pi i \lambda^2 I_{22} = \int_{-\infty}^{\infty} F_2 h \Psi_2 dz = \int_{C_\pm} F_\pm(y) h(y) \Psi_\pm(y) dy , \quad (2.15)$$

for $\pm(\gamma + 1) > 0$, where

$$\begin{aligned}
\Psi_\pm(y) &\equiv c_\pm \sum_{n=1}^{\infty} \frac{\alpha_n^\pm}{y^n} e^{\pm i(y + \alpha \ln y)} , \\
F_\pm(y) &\equiv c_\pm \sum_{n=1}^{\infty} \frac{\tilde{\alpha}_n^\pm}{y^n} e^{\pm i(y + \alpha \ln y)} ,
\end{aligned} \quad (2.16)$$

with

$$c_\pm = \frac{-\pi e^{\pi\alpha/2}}{C\alpha\Gamma(\pm i\alpha)} \exp \left\{ \pm i \left[\frac{-4}{3\lambda^2} + \alpha \ln 2 + z_0 \right] \right\} .$$

The coefficients α_n^\pm and $\tilde{\alpha}_n^\pm$ can be found by substituting the asymptotic series (2.16), making use of Eq. (2.6), into the two differential equations (1.1) and (1.2), requiring that all terms vanish and that they satisfy boundary conditions Eq. (2.2), or (2.3).

The result is

$$\alpha_n^\pm = a_{n,0}^\pm - a_{n,2}^\pm , \quad n \geq 1 ,$$

$$\begin{aligned}
a_{n,0}^{\pm} &= \frac{\pm 1}{2i\lambda^2 n} \left\{ [\alpha \pm i(n-1)] [a_{n-1,3}^{\pm} + a_{n-1,2}^{\pm} + (1+\gamma)a_{n-1,1}^{\pm} + \lambda^2(\alpha \mp in)a_{n-1,0}^{\pm}] \right. \\
&\quad \left. - \sum_{m=1}^{n-1} h_{n-m}^{\pm} \alpha_m^{\pm} \right\}, \\
a_{n,k}^{\pm} &= a_{n,k-1}^{\pm} + [\alpha \pm i(n-1)] a_{n-1,k-1}^{\pm}, \quad k = 1, 2, 3,
\end{aligned} \tag{2.17}$$

and $a_{0,k}^{\pm} = 1$. The calculation for $\tilde{\alpha}_n^{\pm}$ is similar to Eqs. (2.17), with $h_n^{\pm} = 0$. Substituting Eqs. (2.10) and (2.16) into Eq. (2.15), we get

$$2\pi i \lambda^2 I_{22} = c_{\pm}^2 \sum_{n=3}^{\infty} \gamma_n^{\pm} \int_{C_{\pm}} \frac{1}{y^n} e^{\pm 2i(y + \alpha \ln y)} dy, \tag{2.18}$$

for $\pm(\gamma + 1) > 0$, where

$$\begin{aligned}
\gamma_n^{\pm} &= \sum_{m=1}^{n-2} \beta_{n-m}^{\pm} h_m^{\pm}, \quad \text{for } n \geq 3, \\
\beta_n^{\pm} &= \sum_{m=1}^{n-1} \alpha_{n-m}^{\pm} \tilde{\alpha}_m^{\pm}, \quad \text{for } n \geq 2.
\end{aligned}$$

To evaluate the y -integrals in Eq. (2.18), we change the integration contour again. Now, there is only one pole $y = 0$ in the integrand, and there is also a branch cut. We choose the branch cut to be from $y = 0$ to $\pm i\infty$ for the two cases (see Figs. 2.1,2.2). Then we change the integration contours to go along the semicircles with infinite radius at the other side of the real axis, opposite to C_{\pm} , and go around the branch cut (see Figs. 2.1,2.2) so that the analytic continuation is still valid. The contributions from integrating along the two quarters of the semicircles are zero due to the $\exp \pm 2iy$ factor. Integration along the path going around the branch cut can be found by making use of Hankel's contour integral[40],

$$\int_{C_H} (e^{-i\pi t})^{-z} e^{-t} dt = -\frac{2\pi i}{\Gamma(z)}, \tag{2.19}$$

where the contour C_H starts at $t = \infty \exp(0i)$, comes along the positive real axis, turns around the origin counterclockwise, then goes back along the positive real axis

to $t = \infty \exp(2\pi i)$. The y -integral in Eq. (2.18) can be changed to this form by means of a variable transformation $t = 2y \exp(3\pi i/2)$ for $\gamma > -1$, and $t = 2y \exp(\pi i/2)$ for $\gamma < -1$. Thus, we can express I_{22} , or R_2 as a series expression,

$$R_2 = C^2 \pm \frac{i}{2} \left[\frac{\pi T e^{\pm i(z_0 - 4/3\lambda^2)}}{C\alpha\lambda\Gamma(\pm i\alpha)} \right]^2 \sum_{n=3}^{\infty} \frac{\gamma_n^{\pm} (\pm 2i)^n}{\Gamma(n \mp 2i\alpha)}, \quad (2.20)$$

for $\pm(\gamma + 1) > 0$. This expression is analytic in the sense that all coefficients γ_n^{\pm} can be calculated exactly by some algebraic recurrence formula, although they are in general rather lengthy to be written out explicitly. This series is useful only if it is convergent, unless we know how to sum it analytically. However, due to the complicated nature of the coefficients, it is beyond the scope of this dissertation to study the convergence analytically. In the next section, we will present numerical results showing that it does converge, in many cases, to numerically the same values found by solving the integral equation (2.5) iteratively.

Comparisons

We do our calculations explicitly with a deuterium plasma. Table 2.1 to Table 2.3 compare calculations of R_2 for case (i), the second ion cyclotron harmonic with $\gamma > -1$, for different k_{\parallel} and different ranges of λ^2 . P_n is $|R_2|^2$ calculated by solving the integral equation (2.5) iteratively. P_a is that calculated by the series in Eq. (2.20). The values of q_a and q_n , which are defined by $P_a = C^4 \exp(-2q_a\kappa^2)$ and $P_n = C^4 \exp(-2q_n\kappa^2)$, of Table 2.3 are also plotted on Fig. 2.3. Table 2.4 to Table 2.7 compare these for case (ii), the second electron cyclotron harmonic with $\gamma < -1$, where X is the square of the ratio of the plasma frequency to the wave frequency. The values of P_n and P_a of Table 2.4 are also plotted on Fig. 2.4.

$k_{\parallel}(\text{m}^{-1})$	κ	$P_n(\%)$	$P_a(\%)$	q_n	q_a
4	0.09264	2.8208e-2	2.8209e-2	1.0015	1.0000
8	0.1740	1.3145e-2	1.3131e-2	0.9823	1.0000
12	0.2342	3.6283e-3	3.6297e-3	1.0034	1.0000
16	0.2640	5.3536e-4	5.3585e-4	1.0065	1.0000
20	0.2505	2.6688e-5	2.6723e-5	1.0103	1.0000
23	0.1907	3.6852e-7	3.6838e-7	0.9948	1.0000

Table 2.1: Case (i) with large λ^2 , $n_e = 5 \times 10^{19} \text{ m}^{-3}$, $L = 1 \text{ m}$, $B = 6 \text{ T}$, $T_i = 1000 \text{ eV}$.

$k_{\parallel}(\text{m}^{-1})$	κ	$P_n(\%)$	$P_a(\%)$	q_n	q_a
1	0.1337	11.982	11.982	1.0005	0.9994
2	0.2668	10.575	10.578	1.0011	0.9994
3	0.3990	8.6018	8.6084	1.0018	0.9994
4	0.5295	6.4643	6.4747	1.0023	0.9994
5	0.6581	4.5057	4.5167	1.0023	0.9994
6	0.7840	2.9359	2.9353	0.9993	0.9994
7	0.9070	1.7865	1.7864	0.9994	0.9994
8	1.0265	1.0243	1.0243	0.9995	0.9995
9	1.1420	0.55687	0.55704	0.9996	0.9994
10	1.2532	0.28951	0.28936	0.9993	0.9994
11	1.3596	0.14499	0.14467	0.9988	0.9994
12	1.4608	0.070261	0.070179	0.9991	0.9994
13	1.5564	0.033275	0.033298	0.9994	0.9993
14	1.6460	0.015559	0.015581	0.9995	0.9993
15	1.7293	~ 0.01	7.2503e-3	~ 1	0.9992
16	1.8058	diverge	3.3825e-3	diverge	0.9991

Table 2.2: Case (i) with $\lambda^2 \sim 3$, $n_e = 1 \times 10^{20} \text{ m}^{-3}$, $L = 2 \text{ m}$, $B = 3 \text{ T}$, $T_i = 1000 \text{ eV}$.

$k_{\parallel}(\text{m}^{-1})$	κ	$P_n(\%)$	$P_a(\%)$	q_n	q_a
1	0.2837	60.495	60.498	0.9896	0.9893
2	0.5668	37.427	37.432	0.9891	0.9889
3	0.8488	16.903	16.905	0.9881	0.9881
4	1.1292	5.6244	5.6237	0.9862	0.9863
5	1.4073	1.4016	1.4014	0.9826	0.9826
6	1.6828	0.26916	0.27041	0.9759	0.9751
7	1.9550	0.041933	0.043239	0.9639	0.9599
8	2.2234	5.6902e-3	6.4453e-3	0.9450	0.9324
9	2.4875	9.0586e-4	1.0059e-3	0.9014	0.8929
10	2.7468	1.6609e-4	1.6403e-4	0.8497	0.8505
11	3.0009	3.3683e-5	2.4967e-5	0.7986	0.8152
12	3.2492	$\sim 4.e-6$	2.99e-6	~ 0.77	0.794
13	3.4913	diverge	2.1e-7	diverge	0.79

Table 2.3: Case (i) with $\lambda^2 \sim 0.6$, $n_e = 2 \times 10^{20} \text{ m}^{-3}$, $L = 3 \text{ m}$, $B = 3 \text{ T}$, $T_i = 1000 \text{ eV}$.

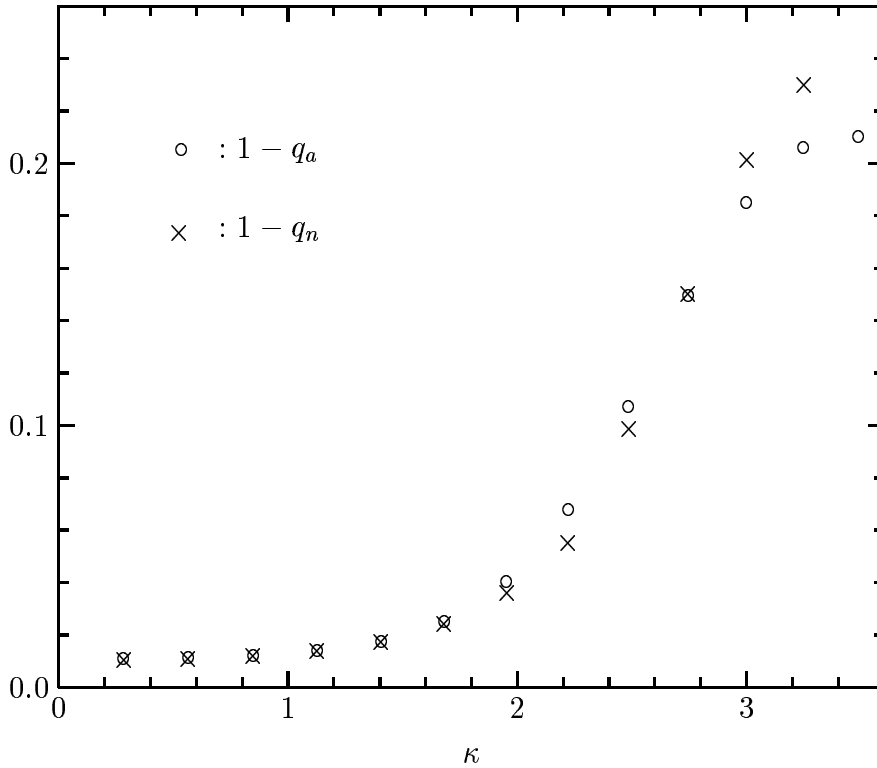


Figure 2.3: Plot of $1 - q_a$ and $1 - q_n$ verse κ , where q_a and q_n are the values in Table 2.3

$T_e(eV)$	λ^2	κ	$P_n(\%)$	$P_a(\%)$	q_n	q_a
50	93.15	0.04736	0.15192	0.15189	6.9114	6.9608
100	46.58	0.09471	0.53250	0.53254	6.8615	6.8574
150	31.05	0.1421	0.99350	0.99340	6.6881	6.6927
200	23.29	0.1894	1.3983	1.3983	6.4770	6.4767
250	18.63	0.2368	1.6648	1.6646	6.2201	6.2212
300	15.53	0.2841	1.7766	1.7755	5.9345	5.9382
350	13.31	0.3315	1.7568	1.7564	5.6381	5.6391
400	11.64	0.3789	1.6496	1.6492	5.3328	5.3336
450	10.35	0.4262	1.4946	1.4941	5.0287	5.0295
500	9.315	0.4736	1.3215	~ 2	4.7341	~ 4
550	8.468	0.5209	1.1503	diverge	4.4494	diverge

Table 2.4: Case (ii) with $X = 0.114$, $n_e = 4 \times 10^{19} \text{ m}^{-3}$, $L = 0.15 \text{ m}$, $B = 3 \text{ T}$.

$T_e(eV)$	λ^2	κ	$P_n(\%)$	$P_a(\%)$	q_n	q_a
5	52.52	0.04800	0.68305	0.68296	6.9240	6.9548
10	26.26	0.09600	2.2822	2.2825	6.8401	6.8341
20	13.13	0.1920	5.4644	5.4662	6.3950	6.3906
30	8.753	0.2880	6.4317	6.4315	5.7674	5.7676
40	6.565	0.3840	5.6863	5.6860	5.0783	5.0785
45	5.836	0.4320	5.0832	5.0833	4.7379	4.7378
50	5.252	0.4800	4.4687	diverge	4.4102	diverge

Table 2.5: Case (ii) with $X = 0.2057$, $n_e = 5 \times 10^{19} \text{ m}^{-3}$, $L = 2 \text{ m}$, $B = 2.5 \text{ T}$.

$T_e(eV)$	λ^2	κ	$P_n(\%)$	$P_a(\%)$	q_n	q_a
50	37.51	0.05154	2.0653	2.0649	6.9021	6.9409
100	18.76	0.1031	6.3723	6.3735	6.7891	6.7799
150	12.50	0.1546	10.456	10.457	6.5280	6.5259
200	9.378	0.2062	12.985	12.988	6.2007	6.1978
250	7.503	0.2577	13.803	13.801	5.8173	5.8181
300	6.252	0.3093	13.357	13.355	5.4087	5.4096
350	5.359	0.3608	12.226	12.224	4.9924	4.9931
400	4.689	0.4124	10.844	10.842	4.5849	4.5854
450	4.168	0.4639	9.4634	~ 9.4	4.1991	~ 4.2
500	3.751	0.5154	8.2082	diverge	3.8395	diverge

Table 2.6: Case (ii) with $X = 0.28575$, $n_e = 1 \times 10^{20} \text{ m}^{-3}$, $L = 0.2 \text{ m}$, $B = 3 \text{ T}$.

T_e (eV)	λ^2	κ	P_n (%)	P_a (%)	q_n	q_a
50	104.6	0.02685	4.6636	4.6634	6.9391	6.9687
250	20.92	0.1342	39.608	39.606	6.3580	6.3596
450	11.62	0.2416	42.896	42.893	5.2409	5.2413
650	8.046	0.3490	33.930	33.930	4.0877	4.0877
850	6.153	0.4564	25.878	25.890	3.1687	3.1676
900	5.811	0.4833	24.249	diverge	2.9804	diverge

Table 2.7: Case (ii) with $X = 0.45725$, $n_e = 1.6 \times 10^{20} \text{ m}^{-3}$, $L = 0.2 \text{ m}$, $B = 3 \text{ T}$.

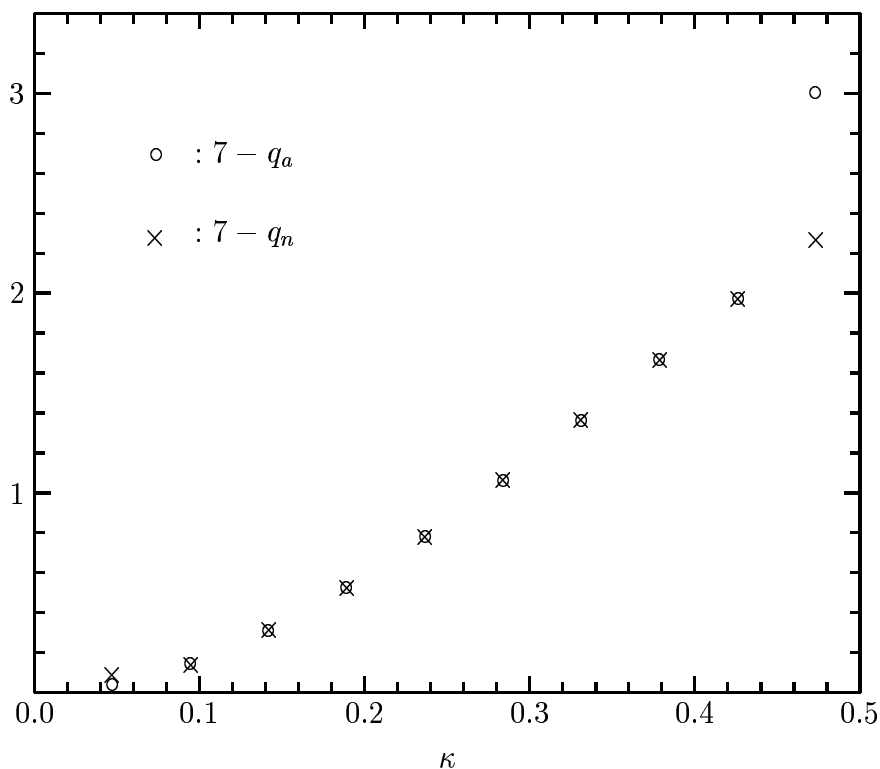


Figure 2.4: Plot of $7 - q_a$ and $7 - q_n$ verse κ , where q_a and q_n are the values in Table 2.4.

Previously, it was found numerically that

$$R_2 \approx C^2 \exp(-q\kappa^2), \begin{cases} \text{with } q \approx 1 & \text{for case (i),} \\ \text{with } q \approx 7 & \text{for case (ii).} \end{cases} \quad (2.21)$$

We see from Table 2.1 to 2.7 that these approximation are very good whenever the condition of large λ^2 , small η , and small κ is satisfied, although it is also good for more general cases. We also list the q_n and q_a values, calculated by each method. The values of q_n and q_a are also plotted in Fig. 3 and Fig. 4.

We first note that these values calculated by both methods agree with each other very well as long as both methods converge. We have also compared results from these two methods for many other cases over a broad range of parameters and they all agree very well. It has been known previously that the iteration method of solving Eq. (2.5) becomes divergent for large absorption (i. e. large κ) for both cases. It seems that the series method using Eq. (2.20) for case (i) is still convergent after the iteration method diverges. However, it also has numerical problems for large κ , due to the fact that we can only sum a finite number of terms and that the computer has a limited power to handle large numbers. On the other hand, the series method becomes divergent faster than the iteration method for case (ii). Actually, it seems that there is a convergence radius of $\kappa < 0.5$ for the series. The reason for this difference is that the asymptotic series of the relativistic plasma dispersion function $F_{\frac{7}{2}}$ of Eq. (2.12) diverges faster than that of the plasma dispersion function Z of Eq. (2.11).

Secondly, we see that the approximation Eq. (2.21) is good, but not exact. Before the development of this series method, the numerical values found by solving the integral equation iteratively were subject to many different kinds of numerical errors, which are difficult to analyze, within the complicated algorithm to calculate f_k and

ψ_κ . Therefore, there was an uncertainty about whether Eq. (2.21) is really exact, and whether the deviations from the rule in the numerical results are just numerical errors. However, now that the series method is analytic in principle, its results are much more reliable and to the extent that they agree with those calculated by the iteration method, this uncertainty no longer exists. Moreover, the series method provides some analytic explanation of Eq. (2.21), at least in extreme cases. Let us consider large λ^2 , small η , and small κ cases. It can be shown by explicitly writing down the first few terms of the series for these cases, using $z_0 = -\gamma/\lambda^2$, that we only need to keep the $n = 3$ terms in the series in Eq. (2.20) to get a good approximation. Note that $\gamma_3^+ = 2\alpha^2\lambda^2\kappa^2$, and $\gamma_3^- = 14\alpha^2\lambda^2\kappa^2$, and using approximations

$$\Gamma(\pm i\alpha) \approx \pm 1/i\alpha, \Gamma(3 \pm 2i\alpha) \approx 2, T \approx 1, C^2 \approx 2\eta,$$

we have

$$\begin{aligned} R_2 &\approx C^2(1 - \kappa^2) \approx C^2 \exp(-\kappa^2) && \text{for case (i) ,} \\ R_2 &\approx C^2(1 - 7\kappa^2) \approx C^2 \exp(-7\kappa^2) && \text{for case (ii) ,} \end{aligned}$$

which is just Eq. (2.21). From numerical calculations, this approximation is very good whenever the condition of large λ^2 , small η , and small κ is satisfied, although it is also good for some more general cases.

Sixth Order Equation

In order to see whether the analytical method developed in the previous section also works for equations with order higher than four, we apply it to a sixth order equation, namely Eq. (1.3). One of the physical situations that this equation can be applied is the third ion cyclotron harmonic[33]. We refer to Ref. [33] for the depen-

dence of the dimensionless parameters, λ^2 , ϵ , γ , z_0 and κ , on the plasma parameters. In the calculation here, we will simply use these dimensionless parameters as inputs.

Similar to the fourth order equation, we can still express the nonzero fast wave reflection coefficient as an integral,

$$R_2 = C^2 \mp I_{22}, \quad \text{for } \pm\alpha > 0,$$

where we still have I_{22} expressed by Eqs. (2.15) and (2.16), but with c_{\pm} being

$$c_{\pm} = \frac{-\pi e^{\pi\alpha/2}}{C\alpha\Gamma(\pm i\alpha)} \exp \left\{ \pm i \left[\frac{-3 - 20\epsilon}{15\lambda^2} + \alpha \ln 2 + z_0 \right] \right\},$$

and

$$\alpha = \frac{\epsilon + \gamma}{2\lambda^2}, \quad T = e^{-\pi|\alpha|}, \quad C^2 = 1 - T^2.$$

The equations to calculate α_n^{\pm} and $\tilde{\alpha}_n^{\pm}$ are similar to Eq. (2.17),

$$\begin{aligned} \alpha_n^{\pm} &= a_{n,0}^{\pm} - a_{n,2}^{\pm}, \quad n \geq 1, \\ a_{n,0}^{\pm} &= \frac{\pm 1}{2i\lambda^2 n} \left\{ [\alpha \pm i(n-1)] [a_{n-1,5}^{\pm} + a_{n-1,4}^{\pm} + \epsilon(a_{n-1,3}^{\pm} + a_{n-1,2}^{\pm}) \right. \\ &\quad \left. + (\epsilon - \lambda^2 z_0)(a_{n-1,1}^{\pm} + a_{n-1,0}^{\pm}) - \lambda^2(\alpha \pm in)a_{n-1,0}^{\pm}] - \sum_{m=1}^{n-1} h_{n-m}^{\pm} \alpha_m^{\pm} \right\}, \\ a_{n,k}^{\pm} &= a_{n,k-1}^{\pm} + [\alpha \pm i(n-1)] a_{n-1,k-1}^{\pm}, \quad k = 2, 3, 4, \end{aligned} \quad (2.22)$$

and $a_{0,k}^{\pm} = 1$. Then, using the same integration technique, the series expression of R_2 can be found

$$R_2 = C^2 \pm \frac{i}{2} \left\{ \frac{\pi T e^{\pm i[z_0 - (3+4\epsilon)/15\lambda^2]}}{C\alpha\lambda\Gamma(\pm i\alpha)} \right\}^2 \sum_{n=3}^{\infty} \frac{\gamma_n^{\pm} (\pm 2i)^n}{\Gamma(n \mp 2i\alpha)}, \quad (2.23)$$

for $\pm\alpha > 0$. Note that this series is very similar to the series Eq. (2.20) of the fourth order equation.

κ	$P_2(\%)$	$P_{3a}(\%)$	$P_{3b}(\%)$	$P_{3c}(\%)$	q_2	q_{3a}
0.1	3.635e-1	3.635e-1	3.635e-1	3.635e-1	0.9999	1.0000
0.3	3.098e-1	3.098e-1	3.098e-1	3.098e-1	0.9999	0.9999
0.6	1.805e-1	1.805e-2	1.805e-2	1.805e-2	0.9999	0.9999
0.9	7.340e-2	7.340e-2	7.340e-2	7.340e-2	0.9999	0.9999
1.2	2.082e-2	2.082e-2	2.082e-2	2.082e-2	0.9999	0.9999
1.5	4.122e-3	4.122e-3	4.122e-3	4.121e-3	0.9999	0.9999
1.8	5.693e-4	5.693e-4	5.694e-4	5.690e-4	0.9999	0.9999
2.1	5.489e-5	5.489e-5	5.490e-5	5.483e-5	0.9998	0.9998
2.4	3.698e-6	3.697e-6	3.701e-6	3.687e-6	0.9996	0.9997
2.7	1.746e-7	1.744e-7	1.750e-7	1.731e-7	0.9992	0.9993
3.0	5.879e-9	5.859e-9	5.931e-9	5.701e-9	0.9978	0.9980
3.5	2.227e-11	2.167e-11	2.413e-11	1.517e-11	0.9607	0.9618
4.0	7.650e-12	7.609e-12	7.807e-12	6.989e-12	0.7689	0.7691
4.5	1.090e-11	1.089e-11	1.091e-11	1.083e-11	0.5988	0.5988
5.0	2.357e-11	1.933e-11	3.350e-11	1.611e-11	0.4696	0.4736
6.0	1.873e-2	3.714e-5	1.688e-4	1.492e-3	0.0415	0.1279

Table 2.8: Comparison of results calculated from Eq. (2.20) and Eq. (2.23) up to 195 terms with $\lambda^2 = 200$, $\alpha = 0.01$ and $z_0 = -\gamma/\lambda^2$. For P_2 and q_2 , $\gamma = 3$; for P_{3a} and q_{3a} , $\epsilon = 1$, $\gamma = 3$; for P_{3b} , $\epsilon = 0.1$, $\gamma = 3.9$; for P_{3c} , $\epsilon = 3.9$, $\gamma = 0.1$.

To compare the results from two series Eqs. (2.20) and (2.23), we consider explicitly using Eq. (2.8) as the absorption function of the fourth order equation and using the negative of it, i. e.,

$$h(z) = -\lambda^2 \kappa [\zeta - 1/Z(-\zeta)] ,$$

as the absorption function of the sixth order equation. The reason for the minus sign is to make sure that both functions represent an absorption problem. We will only use the plasma dispersion function in the calculation because we know from the previous chapter that the series is convergent up to very strong absorption, i. e., large κ . We can then also compare the convergence properties of the two series.

In order to make a reasonable comparison, we need to use the same λ^2 , α and thus T and C values for both cases. However, for Eq. (1.3), $\alpha = (\epsilon + \gamma)/2\lambda^2$, while for

κ	$P_2(\%)$	$P_{3a}(\%)$	$P_{3b}(\%)$	$P_{3c}(\%)$	q_2	q_{3a}
0.1	50.19	50.19	50.19	50.18	0.9777	0.9785
0.3	42.92	42.92	42.93	42.84	0.9773	0.9781
0.6	25.35	25.33	25.36	25.15	0.9758	0.9767
0.9	10.58	10.56	10.60	10.36	0.9730	0.9741
1.2	3.146	3.135	3.158	3.004	0.9684	0.9696
1.5	0.6779	0.6733	0.6830	0.6161	0.9609	0.9624
1.8	0.1095	0.1081	0.1112	9.029e-2	0.9487	0.9506
2.1	1.412e-2	1.381e-2	1.456e-2	9.648e-3	0.9292	0.9317
2.4	1.605e-3	1.550e-3	1.697e-3	7.855e-4	0.9002	0.9032
2.7	1.791e-4	1.709e-4	1.947e-4	5.426e-5	0.8617	0.8649
3.0	2.141e-5	2.029e-5	2.379e-5	4.253e-6	0.8160	0.8189
3.5	1.084e-6	1.043e-6	1.184e-6	3.888e-7	0.7212	0.7228
4.0	4.176e-7	4.167e-7	4.208e-7	3.856e-7	0.5820	0.5821
4.5	5.936e-7	5.940e-7	5.929e-7	5.973e-7	0.4512	0.4512
5.0	8.899e-7	9.031e-7	9.399e-7	9.044e-7	0.3574	0.3571
6.0	0.1302	0.3611	0.08354	0.1725	0.0830	0.0688

Table 2.9: Comparison of results calculated from Eq. (2.20) and Eq. (2.23) up to 195 terms with $\lambda^2 = 20$, $\alpha = 0.2$ and $z_0 = -\gamma/\lambda^2$. For P_2 and q_2 , $\gamma = 7$; for P_{3a} and q_{3a} , $\epsilon = 1$, $\gamma = 7$; for P_{3b} , $\epsilon = 0.1$, $\gamma = 7.9$; for P_{3c} , $\epsilon = 7.9$, $\gamma = 0.1$.

κ	$P_2(\%)$	$P_{3a}(\%)$	$P_{3b}(\%)$	$P_{3c}(\%)$	q_2	q_{3a}
0.1	93.82	93.80	93.83	93.71	0.8592	0.8700
0.3	81.79	81.63	81.93	80.92	0.8575	0.8683
0.6	51.70	51.28	52.08	49.43	0.8515	0.8628
0.9	24.43	23.97	24.89	21.87	0.8411	0.8530
1.2	8.850	8.534	9.191	7.094	0.8257	0.8384
1.5	2.549	2.400	2.728	1.718	0.8051	0.8184
1.8	0.6116	0.5594	0.6828	0.3195	0.7793	0.7931
2.1	0.1282	0.1136	0.1508	4.758e-2	0.7497	0.7634
2.4	2.444e-2	2.102e-2	3.046e-2	6.009e-3	0.7179	0.7310
2.7	4.371e-3	3.665e-3	5.777e-3	6.984e-4	0.6853	0.6974
3.0	7.561e-4	6.222e-4	1.053e-3	8.598e-5	0.6526	0.6634
3.5	4.160e-5	3.443e-5	5.988e-5	6.998e-6	0.5978	0.6055
4.0	6.547e-6	6.435e-6	6.805e-6	5.881e-6	0.5155	0.5160
4.5	9.227e-6	9.339e-6	8.867e-6	9.404e-6	0.3988	0.3985
5.0	1.489e-7	1.507e-7	1.488e-7	1.466e-7	0.3135	0.3132
6.0	5.473e-2	8.765e-2	2.381	0.1116	0.1037	0.0971

Table 2.10: Comparison of results calculated from Eq. (2.20) and Eq. (2.23) up to 195 terms with $\lambda^2 = 3$, $\alpha = 0.6$ and $z_0 = -\gamma/\lambda^2$. For P_2 and q_2 , $\gamma = 2.6$; for P_{3a} and q_{3a} , $\epsilon = 1$, $\gamma = 2.6$; for P_{3b} , $\epsilon = 0.1$, $\gamma = 3.5$; for P_{3c} , $\epsilon = 3.5$, $\gamma = 0.1$.

Eq. (1.2), $\alpha = (1 + \gamma)/2\lambda^2$. So there is an additional parameter for the sixth order equation. The most reasonable comparison is to use $\epsilon = 1$ for Eq. (1.3), because then γ and thus z_0 , which is chosen to be $-\gamma/\lambda^2$ will become the same for both problems. In fact, we will see that the R_2 values have only a weak dependence on ϵ , especially for not so small R_2 .

Table 2.8 to Table 2.10 show data for three ranges of λ^2 . P_2 is $|R_2|^2$ calculated by Eq. (2.20). P_{3a} , P_{3b} and P_{3c} are $|R_2|^2$ calculated by Eq. (2.23) using $\epsilon = 1$, $\epsilon = 0.1$ and $\gamma = 0.1$ respectively. q_2 and q_{3a} are defined by

$$P_2 = C^4 \exp(-2q_2\kappa^2) , \quad P_{3a} = C^4 \exp(-2q_{3a}\kappa^2) .$$

Note that although four figures are shown for the numbers in these tables, not all of them are significant figures, especially for $\kappa > 2.4$, because the convergent rate becomes very slow for large κ . For example, the values for $\kappa = 6$ are obviously not converged since $R_2 \rightarrow 0$ for $\kappa \rightarrow \infty$. However, $|R_2|$ is already so small for $\kappa > 2.4$, this does not affect the application of the series method. We show these values for large κ just to compare the convergence properties of the two series since these values are all calculated by summing up to 195 terms.

From these results, we see that the R_2 values calculated from Eq. (1.3) are very similar to those calculated from Eq. (1.2) even for those highly unconverged values for $\kappa > 4$. The agreement is good for all three choices of ϵ , but especially good for the $\epsilon = 1$ cases since the γ and z_0 values are the same for both series for these cases. However, we can see that the dependence on ϵ is weak, especially for cases with not so small R_2 , which are the only interesting cases practically. The fact that both series give such similar results for the unconverged values after summing up the same number of terms shows that the two series converge in a very similar

way. So the two series have nearly identical convergence properties. Because of this similarity, the empirical formulas Eq. (2.21) are also good approximations for the sixth order equation[33], especially for large λ^2 , small α and κ .

Discussion

The fact that the series method and integral equation method both give essentially the same answers further confirms their own validity respectively, because if either one of these methods is wrong, the chances for their answers to agree with each other accidentally is extremely small.

The success of the series method is amazing and shows how powerful complex analysis can be. In the original form of the integral I_{22} in Eq. (2.7), we needed to know the values of the solutions F_2 , Ψ_2 and the absorption function h along the real z -axis. The straightforward way to do this is first to find $F_2(z)$ by a numerical path integration in the complex plane using the method of Laplace like Eq. (2.1) with a complicated integration and error control scheme. Secondly, solve the integral equation Eq. (2.5) by doing numerical integrations iteratively along the z -axis, with proper end-point corrections, to find $\Psi_2(z)$, making use of numerical methods to evaluate $h(z)$ for z within different regions on the z -axis. Then find I_{22} by numerical integration according to the definition Eq. (2.7). Now, the series method can do the same integration correctly without having to know F_2 , Ψ_2 , and even h on the real z -axis. All it needs is their analytic properties in the complex z -plane and their asymptotic expansions for large complex z values. Also, due to its less complicated algorithm, the series method usually runs much faster on a computer, if we do not care to know the solutions themselves.

This powerful idea may have other applications to solve integrals of similar nature, which arise either from the tunneling problem or other physical problems. After the success on these two relatively simple cases we can try to apply this method for some other more general situations to explore the usefulness of this method. By working on the sixth order three branch problem, we know that the series method also works for higher order mode conversion equations. The results of the sixth order equation are found to be very similar to those of the fourth order equation. Thus, the reflection coefficient R_2 calculated from the fourth order equation can be used as a good approximation of that from the sixth order equation with the same λ^2 , α and κ values for practically interesting cases even when the empirical formulas fail.

ANALYTIC CALCULATIONS OF CERTAIN
SCATTERING PARAMETERS FROM MODE
CONVERSION EQUATIONS

CHAPTER 3

III. FIVE BRANCH PROBLEM

In this chapter, we will first present the integral equations that solve Eq. (1.4) for the \pm cases. We will then show that some fast wave scattering parameters are independent of absorption by considering the solutions in the complex plane. The series method will be applied to calculate C_{23} , C_{32} and R_4 for different cases.

Integral Equations

The homogeneous equation for Eq. (1.4) is

$$f^{vi} + \lambda^2 z [f^{iv} + (1 + k_0^2) f'' + k_0^2 f] + \gamma_2 f'' + \gamma_0 f = 0 .$$

This equation can be solved exactly by using the method of Laplace[4]:

$$f_j(z) = c_j \int_{\Gamma_j} Q(k)^{-1} [\exp z g(k)] dk , \quad (3.1)$$

where the Γ_j are contours in the complex k -plane which must end at infinity with approach angles of $\pi/6$, $5\pi/6$, or $3\pi/2$, and

$$g(k) = -ik - \frac{i}{z} \left\{ S(k) + \sum_{q=1}^4 \alpha_q \ln(k - k_q) \right\} ,$$

with

$$S(k) = -[k^3/3 + (1 + k_0^2)k]/\lambda^2 , \quad Q(k) = (k^2 - 1)(k^2 - k_0^2) ,$$

$$k_1 = -k_2 = 1 , \quad k_3 = -k_4 = k_0 , \quad \alpha_1 = -\alpha_2 , \quad \alpha_3 = -\alpha_4 .$$

We will only consider the two cases (\pm cases) defined before (see Figs. 3.1 and 3.2), and note that the directions of the incident waves of the solutions f_j are indicated by the arrows on the curves. The general contours Γ_j for the two cases are shown in Figs. 3.3 and 3.4. Figs. 3.5 to 3.9 show the contours of asymptotic solutions for some complex z values with $|z| \rightarrow \infty$ for different phase angle θ , where $z = |z| \exp(i\theta)$. We will look at these figures in more detail in the next section. To find the asymptotic behavior of f_j for real z , we can match these general contours to those contours for $z \rightarrow \pm\infty$ which are shown in Figs. 3.5 and 3.9. Then, with a suitable choice of constant c_j , we can express the asymptotic behavior of f_j as

$$\begin{aligned} & \begin{pmatrix} 0 & T_1 & 0 & C_{14} & 0 & C_{16} \\ 1 & R_2 & 0 & C_{24} & 0 & C_{26} \\ 0 & C_{32} & 0 & T_3 & 0 & C_{36} \\ 0 & C_{42} & 1 & R_4 & 0 & C_{46} \\ 0 & C_{52} & 0 & C_{54} & 0 & C_{56} \\ 0 & C_{62} & 0 & C_{64} & 1 & R_6 \end{pmatrix} \begin{pmatrix} u_+ \\ u_- \\ v_+ \\ v_- \\ \sigma_+ \\ \sigma_- \end{pmatrix} \xleftrightarrow{\leftarrow z \rightarrow \infty} \begin{pmatrix} f_1 \\ f_2 \\ f_3 \\ f_4 \\ f_5 \\ f_6 \end{pmatrix} \xrightarrow{z \rightarrow \infty} \\ & \begin{pmatrix} R_1 & 1 & C_{13} & 0 & C_{15} & 0 \\ T_2 & 0 & C_{23} & 0 & C_{25} & 0 \\ C_{31} & 0 & R_3 & 1 & C_{35} & 0 \\ C_{41} & 0 & T_4 & 0 & C_{45} & 0 \\ C_{51} & 0 & C_{53} & 0 & R_5 & 0 \\ C_{61} & 0 & C_{63} & 0 & C_{65} & 1 \end{pmatrix} \begin{pmatrix} u_+ \\ u_- \\ v_+ \\ v_- \\ s_- \\ s_+ \end{pmatrix}, \end{aligned} \quad (3.2)$$

for the $+$ case, and

$$\begin{aligned} & \begin{pmatrix} R_1 & 1 & C_{13} & 0 & 0 & C_{16} \\ T_2 & 0 & C_{23} & 0 & 0 & C_{26} \\ C_{31} & 0 & R_3 & 1 & 0 & C_{36} \\ C_{41} & 0 & T_4 & 0 & 0 & C_{46} \\ C_{51} & 0 & C_{53} & 0 & 0 & C_{56} \\ C_{61} & 0 & C_{63} & 0 & 1 & R_6 \end{pmatrix} \begin{pmatrix} u_- \\ u_+ \\ v_- \\ v_+ \\ \sigma_+ \\ \sigma_- \end{pmatrix} \xleftrightarrow{\leftarrow z \rightarrow \infty} \begin{pmatrix} f_1 \\ f_2 \\ f_3 \\ f_4 \\ f_5 \\ f_6 \end{pmatrix} \xrightarrow{z \rightarrow \infty} \end{aligned}$$

$$\begin{pmatrix} 0 & T_1 & 0 & C_{14} & C_{15} & 0 \\ 1 & R_2 & 0 & C_{24} & C_{25} & 0 \\ 0 & C_{32} & 0 & T_3 & C_{35} & 0 \\ 0 & C_{42} & 1 & R_4 & C_{45} & 0 \\ 0 & C_{52} & 0 & C_{54} & R_5 & 1 \\ 0 & C_{62} & 0 & C_{64} & C_{65} & 0 \end{pmatrix} \begin{pmatrix} u_- \\ u_+ \\ v_- \\ v_+ \\ s_+ \\ s_- \end{pmatrix}, \quad (3.3)$$

for the $-$ case, with scattering parameters given by

$$S_{ij} = \begin{pmatrix} R_1 & T_1 & C_{13} & C_{14} & C_{15} & C_{16} \\ T_2 & R_2 & C_{23} & C_{24} & C_{25} & C_{26} \\ C_{31} & C_{32} & R_3 & T_3 & C_{35} & C_{36} \\ C_{41} & C_{42} & T_4 & R_4 & C_{45} & C_{46} \\ C_{51} & C_{52} & C_{53} & C_{54} & R_5 & C_{56} \\ C_{61} & C_{62} & C_{63} & C_{64} & C_{65} & R_6 \end{pmatrix} = S_{ij}^{(0)},$$

$$S_{ij}^{(0)} = \begin{pmatrix} 0 & T_u & 0 & 0 & -C_u & 0 \\ T_u & T_v^2 C_u^2 & -C_u C_v & T_v C_u C_v & T_u T_v^2 C_u & T_v C_u \\ 0 & -C_u C_v & 0 & T_v & -T_u C_v & 0 \\ 0 & T_v C_u C_v & T_v & C_v^2 & T_u T_v C_v & C_v \\ -C_u & T_u T_v^2 C_u & -T_u C_v & T_u T_v C_v & T_u^2 T_v^2 & T_u T_v \\ 0 & T_v C_u & 0 & C_v & T_u T_v & 1/2 \end{pmatrix}, \quad (3.4)$$

where $T_u = \exp(-\pi|\alpha_1|)$, $T_v = \exp(-\pi|\alpha_3|)$, $C_u^2 = 1 - T_u^2$, $C_v^2 = 1 - T_v^2$ and the six basic waves types are given asymptotically by

$$\begin{aligned} u_{\pm} &\approx \frac{\pi\sqrt{T_u} \exp\{\pm i[S(1) - s_u + z + \alpha_2 \ln|z|]\}}{C_u \alpha_1 (1 - k_0^2) \Gamma(\pm i\alpha_2)}, \\ v_{\pm} &\approx \frac{-\pi\sqrt{T_v} \exp\{\pm i[S(k_0) - s_v + k_0 z + \alpha_4 \ln|z|]\}}{C_v \alpha_3 k_0 (1 - k_0^2) \Gamma(\pm i\alpha_4)}, \\ s_{\pm} &\approx \frac{\text{sgn}(\alpha_2) \sqrt{\pi}}{\lambda^{7/2} z^{9/4}} \exp\left\{\pm i\left[\frac{2}{3}\lambda z^{3/2} - (1 + k_0^2) \frac{z^{1/2}}{\lambda} - \pi/4\right]\right\}, \\ \sigma_+ &\approx \frac{i\sqrt{\pi} e^{\pi(\alpha_1 + \alpha_3)}}{\lambda^{7/2} |z|^{9/4}} \exp\left\{\frac{2}{3}\lambda |z|^{3/2} + (1 + k_0^2) \frac{|z|^{1/2}}{\lambda}\right\}, \\ \sigma_- &\approx \frac{\text{sgn}(\alpha_2) \sqrt{\pi} e^{\pi(\alpha_2 + \alpha_4)}}{\lambda^{7/2} |z|^{9/4}} \exp\left\{-\frac{2}{3}\lambda |z|^{3/2} - (1 + k_0^2) \frac{|z|^{1/2}}{\lambda}\right\}, \end{aligned} \quad (3.5)$$

with

$$s_u = \alpha_1 \ln 2 + \alpha_3 \ln(1 + k_0/1 - k_0), \quad s_v = \alpha_1 \ln(1 + k_0/1 - k_0) + \alpha_3 \ln(2k_0).$$

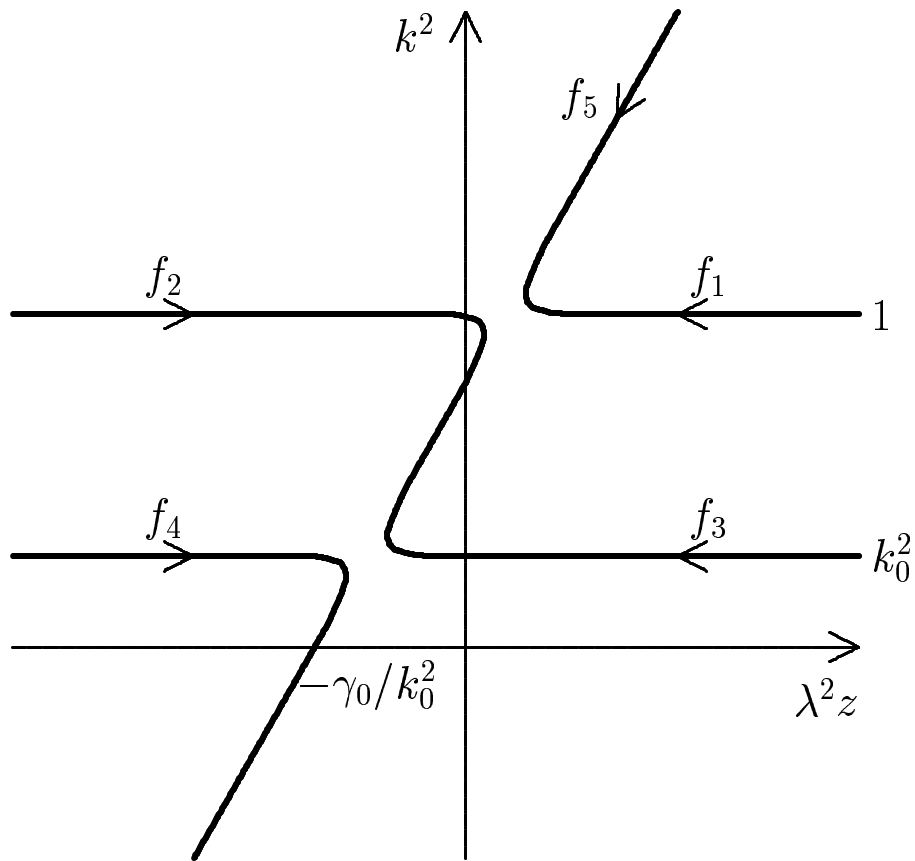


Figure 3.1: Schematic plot of the dispersion relation for the + case.

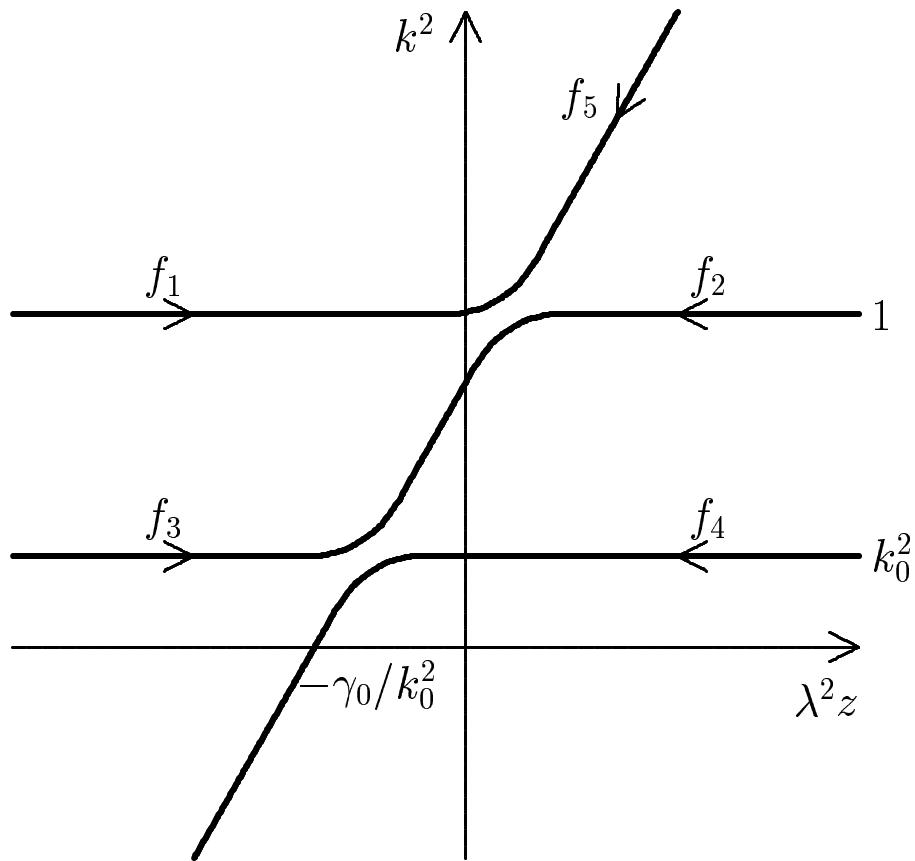


Figure 3.2: Schematic plot of the dispersion relation for the $-$ case.

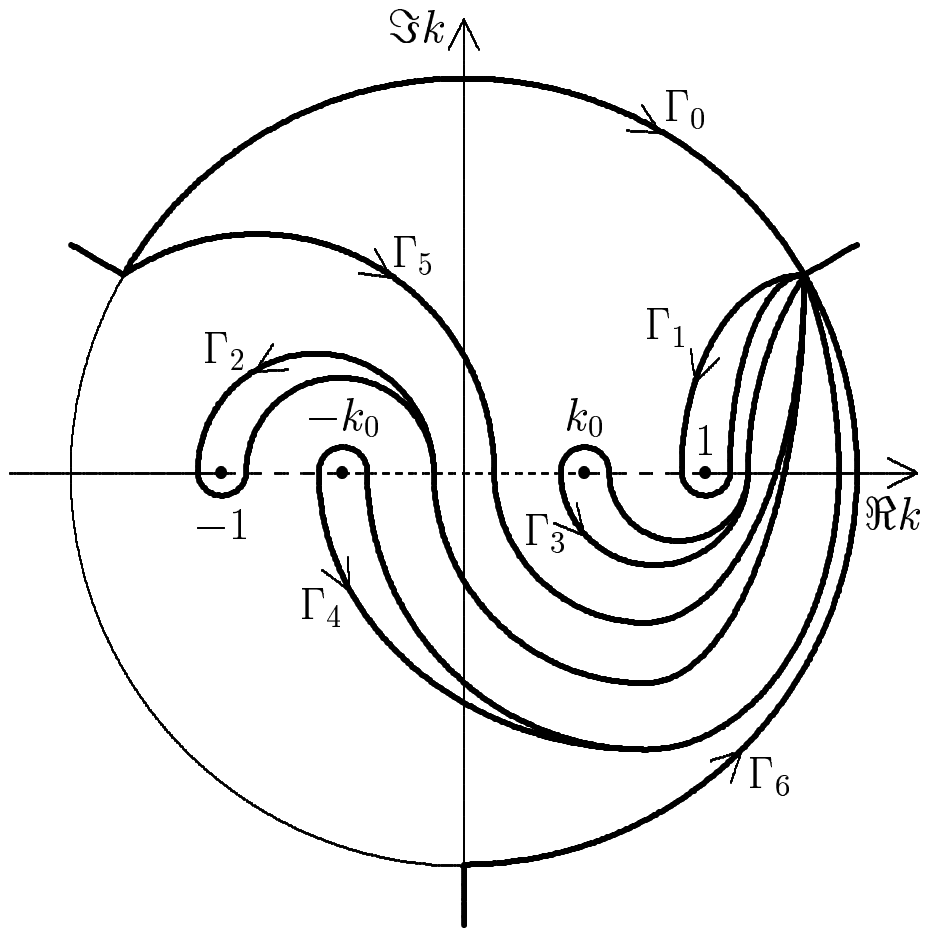


Figure 3.3: General contours of f_j 's for the + case.

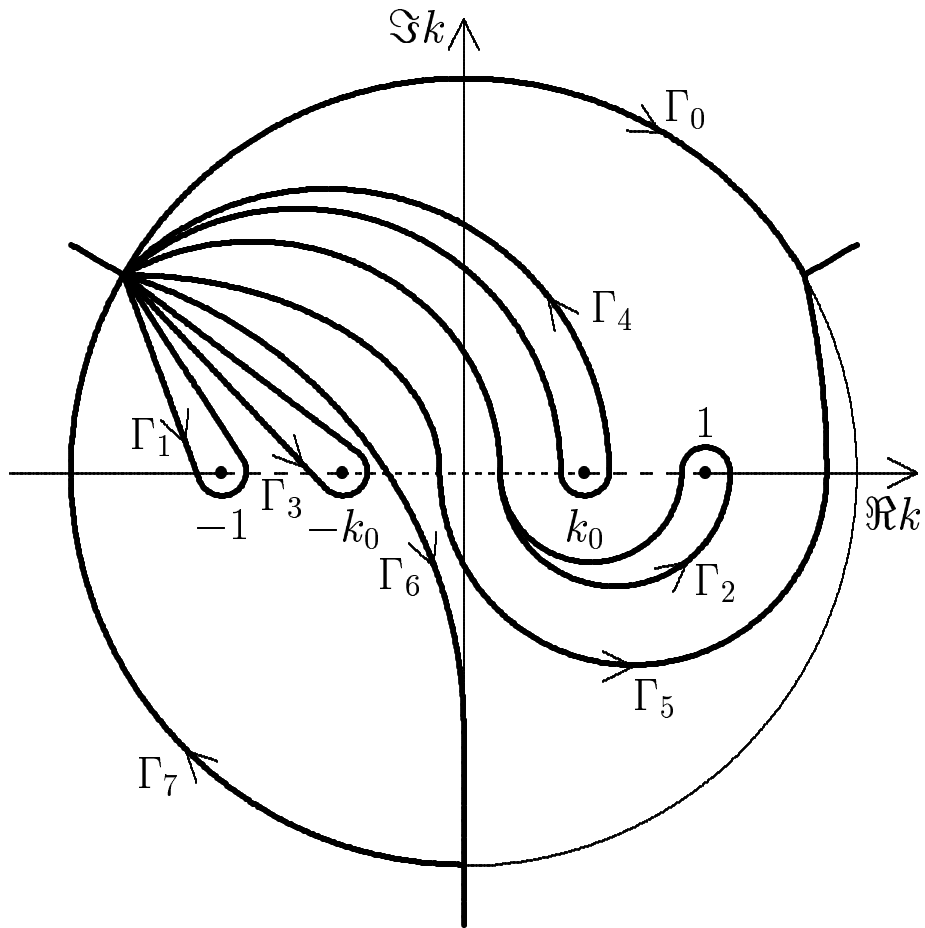


Figure 3.4: General contours of f_j 's for the $-$ case.

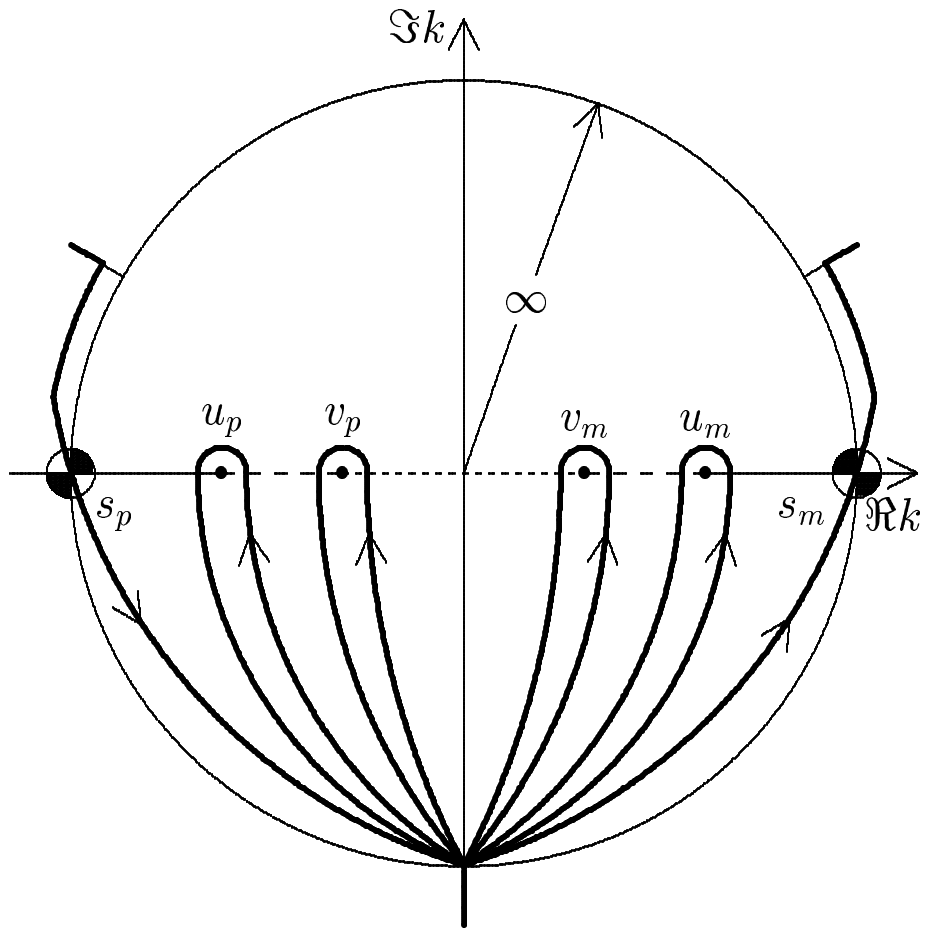


Figure 3.5: Topology of the contours for $z \rightarrow \infty \exp(i\theta)$ with $0 \leq \theta < \theta_1$, plotted for $\theta = 0$.

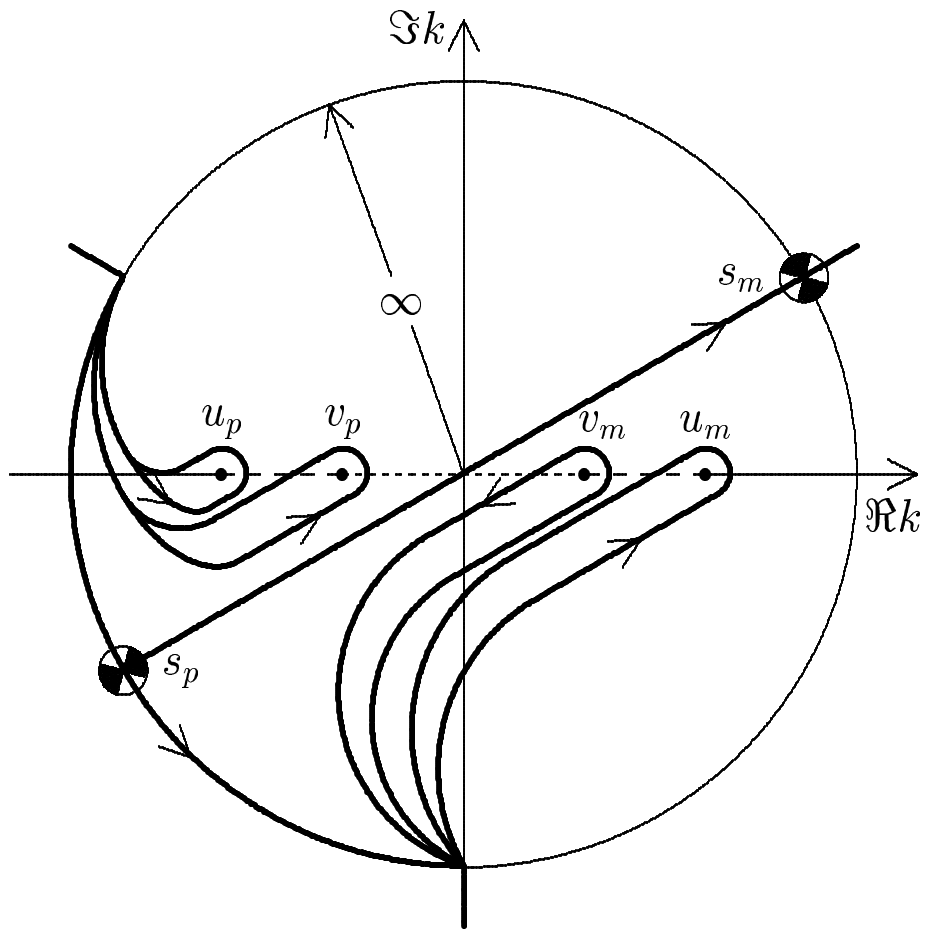


Figure 3.6: Topology of the contours for $z \rightarrow \infty \exp(i\theta)$ with $\theta_1 < \theta < \theta_2$, plotted for $\theta = \pi/3$.

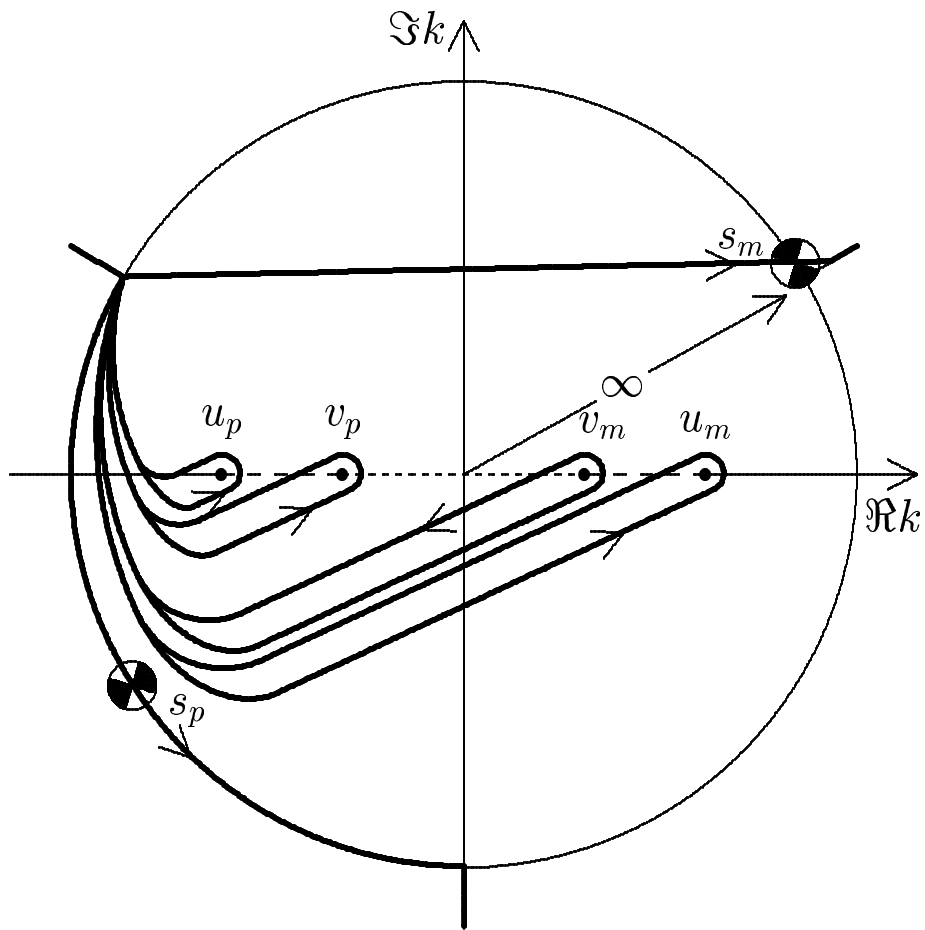


Figure 3.7: Topology of the contours for $z \rightarrow \infty \exp(i\theta)$ with $\theta_2 < \theta < \theta_3$.

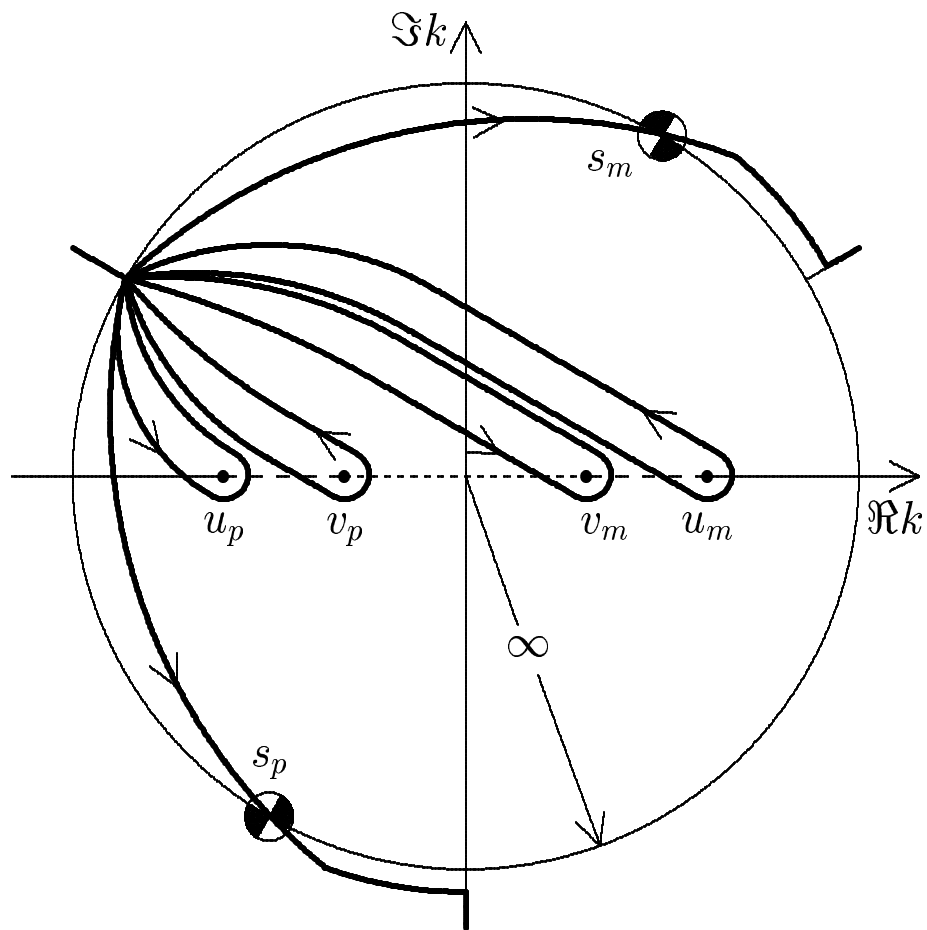


Figure 3.8: Topology of the contours for $z \rightarrow \infty \exp(i\theta)$ with $\theta_3 < \theta < \theta_4$, plotted for $\theta = 2\pi/3$.

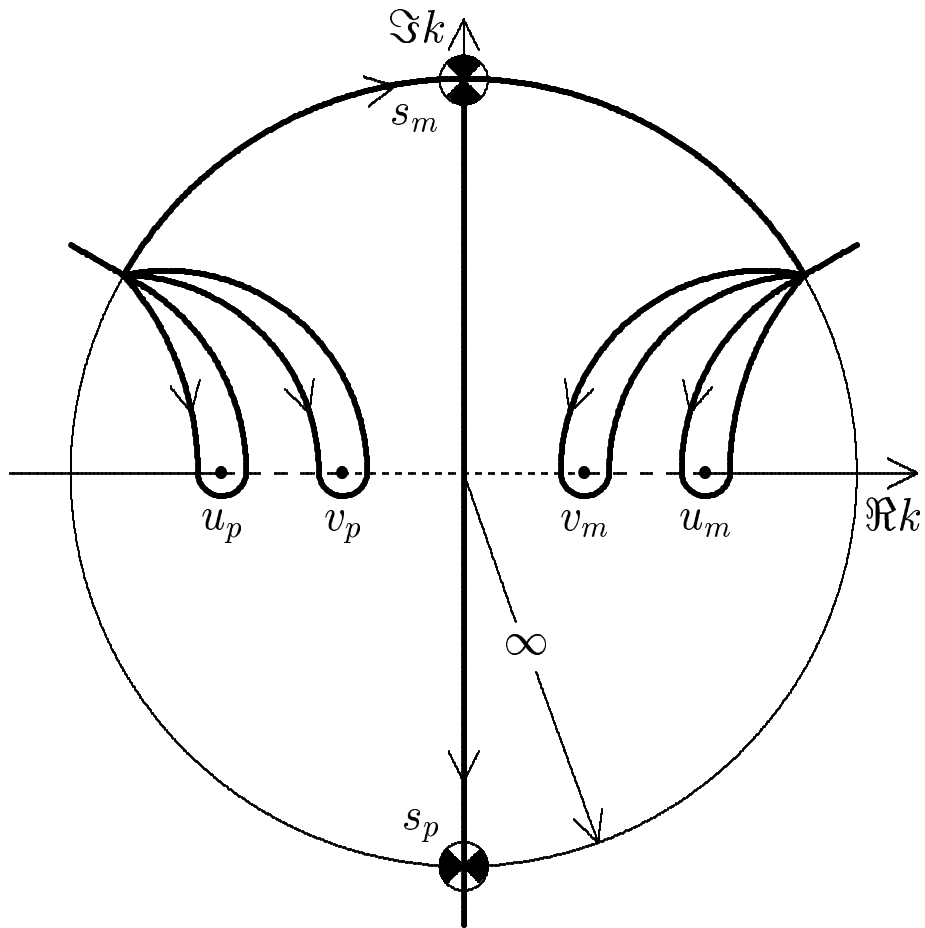


Figure 3.9: Topology of the contours for $z \rightarrow \infty \exp(i\theta)$ with $\theta_4 < \theta \leq \pi$, plotted for $\theta = \pi$.

Note that only f_1 to f_5 are physically allowed in an unbounded region. Using these we can find an integral equation that solves Eq. (1.4),

$$\begin{aligned}
\psi_k &= f_k - \frac{f_2 I_{1k}^-}{T_u} - \frac{f_4 I_{3k}^-}{T_v} - \frac{C_u C_v}{T_u T_v} f_4 I_{1k}^- - f_6 I_{0k}^- \\
&\quad - \frac{f_1 I_{2k}^+}{T_u} - \frac{f_3 I_{4k}^+}{T_v} - \frac{C_u C_v}{T_u T_v} f_1 I_{4k}^+ - f_0 I_{6k}^+, \quad \text{for the + case ,} \\
\psi_k &= f_k + \frac{f_1 I_{2k}^-}{T_u} + \frac{f_3 I_{4k}^-}{T_v} + \frac{C_u C_v}{T_u T_v} f_1 I_{4k}^- + f_7 I_{0k}^- \\
&\quad + \frac{f_2 I_{1k}^+}{T_u} + \frac{f_4 I_{3k}^+}{T_v} + \frac{C_u C_v}{T_u T_v} f_4 I_{1k}^+ + f_0 I_{7k}^+, \quad \text{for the - case ,} \quad (3.6)
\end{aligned}$$

where

$$I_{jk}^\pm = \frac{\pm 1}{2\pi i \lambda^2} \int_z^{\pm\infty} F_j(y) h(y) \Psi_k(y) dy ,$$

with

$$F_j = f_j^{iv} + (1 + k_0^2) f_j'' + k_0^2 f_j , \quad \Psi_j = \psi_j^{iv} + (1 + k_0^2) \psi_j'' + k_0^2 \psi_j , \quad (3.7)$$

and $T_u T_v f_0 \equiv f_5 - T_u C_v f_3 - C_u f_1$ for the + case, and $f_0 \equiv T_u T_v f_5 + T_v C_u f_2 + C_v f_4$, $f_7 \equiv f_6 - C_u f_1 / T_u T_v - C_v f_3 / T_v$ for the - case. Note that $f_0 \rightarrow \sigma_-$ as $z \rightarrow -\infty$ for both cases. Eq. (3.6) can be solved iteratively using $\psi_k = f_k$ as the first trial function with f_k calculated numerically by Eq. (3.1). This can be done for the five physical solutions, $k = 1, 2, 3, 4, 5$, if $h(z)$ falls off at least as fast as z^{-1} as $|z| \rightarrow \infty$. For the $k = 6$ solution, this can be done only if $h(z)\sigma_+(z) \rightarrow 0$ fast enough as $z \rightarrow -\infty$. After solving Eq. (3.6), scattering parameters can be found, making use of Eqs. (3.2)–(3.4), by

$$S_{jk} = S_{jk}^{(0)} \mp I_{kj} = S_{jk}^{(0)} \mp I_{jk} , \quad \text{for } \pm \text{ cases ,} \quad (3.8)$$

with

$$I_{jk} = \frac{1}{2\pi i \lambda^2} \int_{-\infty}^{\infty} F_j(z) h(z) \Psi_k(z) dz , \quad (3.9)$$

where the second equality in Eq. (3.8) is by a reciprocity relation $I_{jk} = I_{kj}$ which can be proved from the symmetric properties of the integral equations[36]. From Eqs. (3.4) and (3.8), we see that $S_{jk} = S_{kj}$ is a symmetric matrix. In the following sections, we will show how some of these I_{jk} are identically zero for some kinds of h functions, and thus some scattering parameters are independent of absorption and can be expressed by Eq. (3.4).

Solutions for Complex z

One possible way to evaluate I_{jk} of Eq. (3.9) is to perform the integration in the complex z -plane. This can be done only if the h function has some good analytical properties in the z -plane. We will assume that h is analytic and tends to zero at least as fast as $|z|^{-1}$ for z on or below (above) the real axis for the $+$ ($-$) case. Also, it has been shown that F_j and Ψ_j are analytic everywhere[24]. Then we can change the path of integration of I_{jk} , defined as the semicircles C_{\pm} in Figs. 2.1 and 2.2,

$$I_{jk} = \frac{1}{2\pi i \lambda^2} \int_{C_{\pm}} F_j(z) h(z) \Psi_k(z) dz, \quad (3.10)$$

with $y \equiv z - z_0$ on the figures for later convenience. The solutions f_j for complex z values are still defined by Eq. (3.1) with the same integration contours. The asymptotic behavior of the f_j on C_{\pm} can be found by considering the contours of asymptotic solutions for $z \rightarrow \infty \exp i\theta$, with $-\pi < \theta < 0$ for the $+$ case and $0 < \theta < \pi$ for the $-$ case, see Figs. 2.1 and 2.2. Let us look at the $-$ case first. After some consideration, one realizes that there are five regions of θ where these contours are topologically different. These five regions are $0 \leq \theta < \theta_1$, $\theta_1 < \theta < \theta_2$, $\pi/3 < \theta_2 < \theta < \pi/2 \equiv \theta_3$, $\theta_3 < \theta < \theta_4 > 2\pi/3$, and $\theta_4 < \theta \leq \pi$, see Figs. 3.5 to 3.9.

The exact values of θ_1 to θ_4 are not important to the proof here except the fact that $\theta_4 > 2\pi/3$, which can be quite obviously seen from these figures. Note that the asymptotic solutions indicated on these figures have the following asymptotic behavior,

$$\begin{aligned} u_p &\propto e^{iz} \downarrow, & u_m &\propto e^{-iz} \uparrow, \\ v_p &\propto e^{ik_0z} \downarrow, & v_m &\propto e^{-ik_0z} \uparrow, \\ s_p &\propto e^{i\frac{2}{3}\lambda z^{3/2}} \begin{cases} \downarrow & 0 < \theta < 2\pi/3 \\ \uparrow & 2\pi/3 < \theta < \pi \end{cases}, \\ s_m &\propto e^{-i\frac{2}{3}\lambda z^{3/2}} \begin{cases} \uparrow & 0 < \theta < 2\pi/3 \\ \downarrow & 2\pi/3 < \theta < \pi \end{cases}, \end{aligned}$$

where \uparrow indicates that it is an exponentially growing solution and \downarrow indicates that it is an exponentially decaying solution.

The circles on these figures, with the four quarters being black and white alternately, indicate the saddle points of the two slow wave asymptotic solutions. The white quarters represent the downhill sides and the black quarters represent the uphill sides. The positions of these two saddle points for $z = |z| \exp(i\theta)$ are

$$k_s = \pm \lambda z^{1/2} = \pm \lambda |z|^{1/2} e^{i\theta/2},$$

with crossing angles ϕ determined by

$$2\phi + \frac{\theta}{2} = \pm \frac{\pi}{2}.$$

Note that ϕ of each circle on these figures is just the angle of the middle line that divides the circle into two symmetric parts along the two white quarters. We see that the slow wave saddle points tend to infinity as $|z| \rightarrow \infty$, i.e. for z on the contour C_- .

The fast wave asymptotic solutions can be calculated by using Hankel's contour integral Eq. (2.19). The contour of each fast wave has to go around a fast wave branch point k_q , $q = 1, 2, 3$ or 4 , that comes in along a direction on which

$$k - k_q = |k - k_q| e^{-i\theta - i\pi/2} ,$$

and goes out along a direction on which

$$k - k_q = |k - k_q| e^{-i\theta + 3i\pi/2} .$$

These directions are also indicated by the shape of the fast wave contours on Figs. 3.5 to 3.9. This means that these four fast wave contours have to turn 180 degrees as θ changes from 0 to π .

By comparing the topology of the general contours in Fig. 3.4 to those contours in Figs. 3.5 to 3.9, we can find out the asymptotic behavior of f_j . For $0 < \theta < \theta_1$ (see Fig. 3.5),

$$\begin{aligned}
f_1 &\propto s_p \rightarrow u_p \rightarrow -s_p \propto u_p \downarrow , \\
f_2 &\propto s_p \rightarrow -u_p \rightarrow -v_p \rightarrow u_m \rightarrow v_p \rightarrow u_p \rightarrow -s_p \propto u_m \uparrow , \\
f_3 &\propto s_p \rightarrow -u_p \rightarrow v_p \rightarrow u_p \rightarrow -s_p \propto v_p \downarrow , \\
f_4 &\propto s_p \rightarrow -u_p \rightarrow -v_p \rightarrow v_m \rightarrow v_p \rightarrow u_p \rightarrow -s_p \propto v_m \uparrow , \\
f_5 &\propto s_p \rightarrow -u_p \rightarrow -v_p \rightarrow s_m \propto s_m \uparrow , \\
f_7 &\propto -s_p \downarrow , \\
f_0 &\propto s_p \rightarrow -u_p \rightarrow -v_p \rightarrow -v_m \rightarrow -u_m \rightarrow s_m \propto s_m \uparrow , \quad (3.11)
\end{aligned}$$

where the \rightarrow indicates the order of going through these paths so that the contours of the individual solutions will be added up to be topologically equal to the the

general contour for each solution f_j . We did not show proportional constants which are not important in the discussion here, although they are important in getting the scattering parameters of Eqs. (3.2) to (3.4). For $\theta_1 < \theta < \theta_2$ (see Fig. 3.6),

$$\begin{aligned}
f_1 &\propto u_p \downarrow , \\
f_2 &\propto -u_p \rightarrow -v_p \rightarrow s_p \rightarrow u_m \rightarrow -s_p \rightarrow v_p \rightarrow u_p \propto u_m \uparrow , \\
f_3 &\propto -u_p \rightarrow v_p \rightarrow u_p \propto v_p \downarrow , \\
f_4 &\propto -u_p \rightarrow -v_p \rightarrow s_p \rightarrow v_m \rightarrow -s_p \rightarrow v_p \rightarrow u_p \propto v_m \uparrow , \\
f_5 &\propto -u_p \rightarrow -v_p \rightarrow s_p \rightarrow u_m \rightarrow v_m \rightarrow -s_p/2 \rightarrow s_m \propto s_m \uparrow , \\
f_7 &\propto -s_p \downarrow , \\
f_0 &\propto -u_p \rightarrow -v_p \rightarrow s_p/2 \rightarrow s_m \propto s_m \uparrow .
\end{aligned} \tag{3.12}$$

For $\pi/3 < \theta_2 < \theta < \pi/2 \equiv \theta_3$ (see Fig. 3.7),

$$\begin{aligned}
f_1 &\propto u_p \downarrow , \\
f_2 &\propto -u_p \rightarrow -v_p \rightarrow u_m \rightarrow v_p \rightarrow u_p \propto u_m \uparrow , \\
f_3 &\propto -u_p \rightarrow v_p \rightarrow u_p \propto v_p \downarrow , \\
f_4 &\propto -u_p \rightarrow -v_p \rightarrow v_m \rightarrow v_p \rightarrow u_p \propto v_m \uparrow , \\
f_5 &\propto -u_p \rightarrow -v_p \rightarrow u_m \rightarrow v_m \rightarrow v_p \rightarrow u_p \rightarrow s_m \propto s_m \uparrow , \\
f_7 &\propto -s_p \downarrow , \\
f_0 &\propto s_m \uparrow .
\end{aligned} \tag{3.13}$$

For $\theta_3 < \theta < \theta_4$, see Fig. 3.8,

$$\begin{aligned}
f_1 &\propto u_p \downarrow , \\
f_2 &\propto v_m \rightarrow u_m \rightarrow -v_m \propto v_m + u_m \uparrow ,
\end{aligned}$$

$$\begin{aligned}
f_3 &\propto v_p \downarrow , \\
f_4 &\propto v_m \uparrow , \\
f_5 &\propto v_m \rightarrow u_m \rightarrow s_m \propto \begin{cases} s_m \uparrow & \theta < 2\pi/3 \\ u_m \uparrow & \theta > 2\pi/3 \end{cases} , \\
f_7 &\propto -s_p \begin{cases} \downarrow & \theta < 2\pi/3 \\ \uparrow & \theta > 2\pi/3 \end{cases} , \\
f_0 &\propto s_m \begin{cases} \uparrow & \theta < 2\pi/3 \\ \downarrow & \theta > 2\pi/3 \end{cases} .
\end{aligned} \tag{3.14}$$

For $\theta_4 < \theta < \pi$, see Fig. 3.9,

$$\begin{aligned}
f_1 &\propto u_p \downarrow , \\
f_2 &\propto s_m \rightarrow v_m \rightarrow u_m \rightarrow -v_m \rightarrow -s_m \propto v_m + u_m \uparrow , \\
f_3 &\propto v_p \downarrow , \\
f_4 &\propto s_m \rightarrow v_m \rightarrow -s_m \propto v_m \uparrow , \\
f_5 &\propto s_m \rightarrow v_m \rightarrow u_m \propto u_m \uparrow , \\
f_7 &\propto -s_p \rightarrow -s_m/2 \rightarrow -v_p \rightarrow -u_p \propto -s_p \uparrow , \\
f_0 &\propto s_m \downarrow .
\end{aligned} \tag{3.15}$$

In summary, the asymptotic behavior of the fast wave solutions f_1 to f_4 for z on the contours C_- are

$$\begin{aligned}
f_1 &\propto u_p \propto e^{iz} \downarrow , \\
f_2 &\propto u_m \propto e^{-iz} \uparrow , \\
f_3 &\propto v_p \propto e^{ik_0z} \downarrow , \\
f_4 &\propto v_m \propto e^{-ik_0z} \uparrow .
\end{aligned} \tag{3.16}$$

By Eq. (3.7), it is obvious that F_j has the same asymptotic behavior as f_j . To show that ψ_j , and thus Ψ_j has the same asymptotic behavior as f_j , we need to define ψ_j for complex z values using the integral equation (3.6). By redefining the end points of some of the integrals in Eq. (3.6), namely end points of $I_{41}^-, I_{11}^+, I_{31}^+, I_{13}^+, I_{33}^+, I_{14}^+$

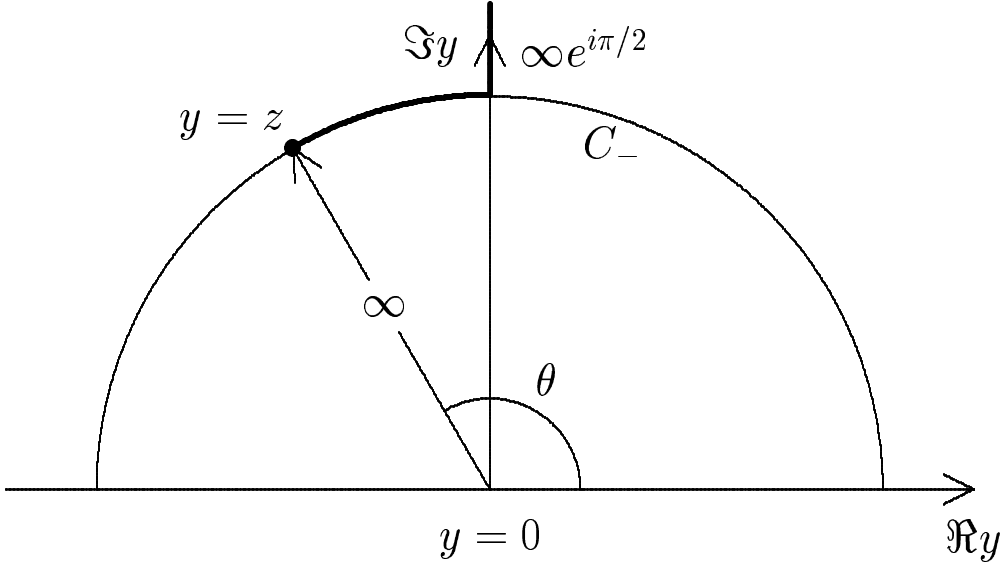


Figure 3.10: Integration contours on the complex plane for some of the $I_{jk}^{\pm}(z)$ of fast waves for the $-$ case.

changed to $\infty e^{i\pi/2}$ (see Fig. 3.10), and end points of I_{7k}^+ with $k = 1, 2, 3, 4$ changed to $\infty e^{i\pi/3}$ (see Fig. 3.11), it can be shown that the ψ_k in the left hand side of Eq. (3.6) will have the same asymptotic behavior as f_k , provided that the Ψ_k on the right hand side of Eq. (3.6) is assumed to have this property. This can be seen by considering the asymptotic behavior of each term of the right hand side of Eq. (3.6) for each k . Note that these redefinitions of end points will not affect the values of ψ_k for z on the real axis. So, Ψ_k indeed has the same asymptotic behavior as f_k , for $k = 1, 2, 3, 4$, if the integral equation (3.6) is convergent for these solutions. This will be true if $h \rightarrow 0$ at least as fast as $|z|^{-1}$, as assumed. Note that the fact that $f_7 \propto s_p$ and $f_0 \propto s_m$ for z on C_- has been used in this proof.

For the $+$ case, the integration contour is changed to C_+ defined in Fig. 2.1. There are also five regions of θ where the contours of the asymptotic solutions are topologically different. These five regions are $0 \geq \theta > -\theta_1$, $-\theta_1 > \theta > \theta_2$, $-\theta_2 > \theta > -\theta_3$, $-\theta_3 > \theta > -\theta_4$, and $-\theta_4 > \theta \geq -\pi$. The contours for this case

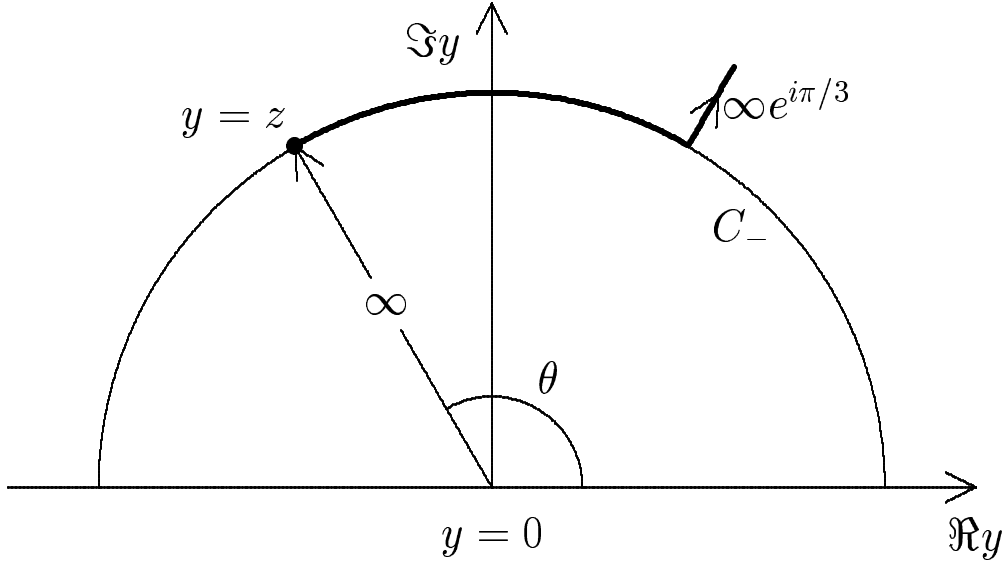


Figure 3.11: Integration contours on the complex plane of $I_{7k}^+(z)$ for $k = 1, 2, 3, 4$ of the $-$ case.

are symmetric to those in Figs. 3.5 to 3.9, so we will not show them here, but will point out an easy way to get them from these figures. We only need to make a mirror reflection about the imaginary k -axis of those contours in Figs. 3.5 to 3.9, then exchange the labels $m \leftrightarrow p$, and change the directions of the arrows to the opposite. Then the asymptotic behavior of f_k can be found for each region. For $0 > \theta > -\theta_1$,

$$\begin{aligned}
 f_1 &\propto -s_m \rightarrow u_m \rightarrow s_m \propto u_m \downarrow , \\
 f_2 &\propto -s_m \rightarrow v_p \rightarrow u_p \rightarrow -v_p \rightarrow -v_m \rightarrow s_m \propto v_p + u_p \uparrow , \\
 f_3 &\propto -s_m \rightarrow v_m \rightarrow s_m \propto v_m \downarrow , \\
 f_4 &\propto -s_m \rightarrow v_p \rightarrow s_m \propto v_p \uparrow , \\
 f_5 &\propto s_p \rightarrow -v_p \rightarrow -u_p \rightarrow s_m \propto s_p \uparrow , \\
 f_6 &\propto s_m \downarrow , \\
 f_0 &\propto s_p \rightarrow -u_p \rightarrow -v_p \rightarrow -v_m \rightarrow -u_m \rightarrow s_m \propto s_p \uparrow . \quad (3.17)
 \end{aligned}$$

For $-\theta_1 > \theta > -\theta_2$,

$$\begin{aligned}
f_1 &\propto u_m \downarrow , \\
f_2 &\propto -s_m \rightarrow v_p \rightarrow u_p \rightarrow -v_p \rightarrow -s_m \propto v_p + u_p \uparrow , \\
f_3 &\propto v_m \downarrow , \\
f_4 &\propto -s_m \rightarrow v_p \rightarrow s_m \propto v_p \uparrow , \\
f_5 &\propto s_p \rightarrow s_m/2 \rightarrow s_p \propto s_p \uparrow , \\
f_6 &\propto s_m \downarrow , \\
f_0 &\propto s_p \rightarrow s_m/2 \rightarrow -v_m \rightarrow -u_m \propto s_p \uparrow .
\end{aligned} \tag{3.18}$$

For $-\theta_2 > \theta > -\theta_3$,

$$\begin{aligned}
f_1 &\propto u_m \downarrow , \\
f_2 &\propto v_p \rightarrow u_p \rightarrow -v_p \propto v_p + u_p \uparrow , \\
f_3 &\propto v_m \downarrow , \\
f_4 &\propto v_p \uparrow , \\
f_5 &\propto s_p \rightarrow u_m \rightarrow v_m \rightarrow s_p \propto s_p \uparrow , \\
f_6 &\propto s_m \downarrow , \\
f_0 &\propto s_p \uparrow .
\end{aligned} \tag{3.19}$$

For $-\theta_3 > \theta > -\theta_4$,

$$\begin{aligned}
f_1 &\propto u_m \downarrow , \\
f_2 &\propto -u_m \rightarrow -v_m \rightarrow u_p \rightarrow v_m \rightarrow u_m \propto u_p \uparrow , \\
f_3 &\propto -u_m \rightarrow v_m \rightarrow u_m \propto v_m \downarrow , \\
f_4 &\propto -u_m \rightarrow -v_m \rightarrow v_p \rightarrow v_m \rightarrow u_m \propto v_p \uparrow ,
\end{aligned}$$

$$\begin{aligned}
f_5 &\propto s_p \rightarrow v_m \rightarrow u_m \propto \begin{cases} s_p \uparrow & \theta > -2\pi/3 \\ v_m \downarrow & \theta < -2\pi/3 \end{cases} , \\
f_6 &\propto s_m \begin{cases} \downarrow & \theta > -2\pi/3 \\ \uparrow & \theta < -2\pi/3 \end{cases} , \\
f_0 &\propto s_p \begin{cases} \uparrow & \theta > -2\pi/3 \\ \downarrow & \theta < -2\pi/3 \end{cases} .
\end{aligned} \tag{3.20}$$

For $-\theta_4 > \theta > -\pi$,

$$\begin{aligned}
f_1 &\propto u_m \downarrow , \\
f_2 &\propto -u_m \rightarrow -v_m \rightarrow -s_p \rightarrow u_p \rightarrow s_p \rightarrow v_m \rightarrow u_m \propto u_p \uparrow , \\
f_3 &\propto -u_m \rightarrow v_m \rightarrow u_m \propto v_m \downarrow , \\
f_4 &\propto -u_m \rightarrow -v_m \rightarrow -s_p \rightarrow v_p \rightarrow s_p \rightarrow v_m \rightarrow u_m \propto v_p \uparrow , \\
f_5 &\propto s_p \rightarrow v_m \rightarrow u_m \propto v_m \downarrow , \\
f_6 &\propto s_m \rightarrow s_p/2 \rightarrow v_m \rightarrow u_m \propto s_m \uparrow , \\
f_0 &\propto s_p \downarrow .
\end{aligned} \tag{3.21}$$

In summary, the asymptotic behavior of the fast wave solutions f_1 to f_4 for z on the contours C_+ are

$$\begin{aligned}
f_1 &\propto u_m \propto e^{-iz} \downarrow , \\
f_2 &\propto u_p \propto e^{iz} \uparrow , \\
f_3 &\propto v_m \propto e^{-ik_0z} \downarrow , \\
f_4 &\propto v_p \propto e^{ik_0z} \uparrow .
\end{aligned} \tag{3.22}$$

Using similar arguments, it can be shown that F_k and Ψ_k have the same asymptotic behavior as f_k , for $k = 1, 2, 3, 4$.

Scattering Parameters

Independence of Absorption

By the definition of I_{jk} in Eq. (3.10), where we have use the assumption that h is analytic on or below (above) the real axis for the $+$ ($-$) case and the fact that F_j and Ψ_j are analytic everywhere, and the asymptotic behavior of Ψ_k and F_j , described by Eqs. (3.16) and (3.22), on the contours C_{\pm} for the two cases, we know immediately that for certain reflection (I_{jj}) and conversion coefficients,

$$I_{11} = I_{33} = I_{13} = I_{31} = I_{14} = I_{41} = 0 .$$

Note that h function for all the physical situations we consider here satisfy these assumptions, because $Z(\zeta)$ and $F_q(\zeta)$ are analytic functions and have zeros only in the upper ζ -plane.

Using the fact that on C_{\pm} , $h \sim \mathcal{O}(|z|^{-1})$, and

$$F_k \sim \mathcal{O}(|z|^{-1} f_k) ,$$

for $k = 1, 2, 3, 4$, by Eqs. (3.5) and (3.7), we also know that for all of the fast wave transmission coefficients,

$$I_{12} = I_{21} = I_{34} = I_{43} = 0 .$$

Then from the relations of the scattering parameters with I_{jk} in Eq. (3.8), using Eq. (3.4), we can find certain fast wave scattering parameters analytically, namely:

$$T_1 = T_2 = T_u ,$$

$$T_3 = T_4 = T_v ,$$

$$R_1 = R_3 = C_{13} = C_{31} = C_{14} = C_{41} = 0 .$$

Obviously, these scattering parameters are independent of absorption. However, the conversion coefficient $C_{23}(= C_{32})$ which has been found numerically to be independent of absorption is not one of these. So we need to calculate it by another method.

Series Method

In this section, we will apply the analytical method to find the series expressions for some of these nonzero fast wave scattering parameters. The correctness of this method has been shown by the very good agreement between the results from the series method and the integral equation method in calculating the nonzero fast wave reflection coefficient from Eq. (1.2) in Chapter II. The derivation here will be very similar there and we refer to it for details that are omitted here.

Since we need to perform explicit calculations in this section, we need to specify the absorption function h . We will consider two kinds of function that appear frequently in physical situations. For the nonrelativistic cases, we use

$$h(z) = \lambda^2 \kappa [\zeta \mp 1/Z(\pm\zeta)] , \quad (3.23)$$

for \pm cases, and for relativistic cases from Eq. (1.4),

$$h(z) = \lambda^2 \kappa \left[\zeta \pm 1/F_{\frac{7}{2}}(\mp\zeta - 7/2) \right] , \quad (3.24)$$

and for the relativistic cases from Eq. (1.6),

$$h(z) = -\lambda^2 \kappa \left[\zeta \pm 1/F_{\frac{9}{2}}(\mp\zeta - 9/2) \right] . \quad (3.25)$$

Note again that both $Z(\zeta)$, $F_{\frac{7}{2}}(\zeta)$ and $F_{\frac{9}{2}}(\zeta)$ are analytic functions and have zeros only in the lower half ζ -plane. We will also assume that $z_0 = -\gamma_0/k_0^2\lambda^2$, which is

often the case for physical situations. We refer to Refs. [34, 35, 36] for the dependence on plasma parameters of the dimensionless parameters $\lambda^2, \gamma_6, \gamma_2, \gamma_0, k_0,$ and κ . In the calculations here, we will use these dimensionless parameters as inputs so that the conclusions are not restricted to a particular physical situation.

First we need to expand $h(z)$ in an asymptotic series over C_{\pm} for the two cases,

$$h(z) \rightarrow \sum_{n=1}^{\infty} \frac{h_n}{y^n} .$$

We have already shown a general method to do so, for those functions of Eqs.(3.23)–(3.25), in Chapter II.

For the mode conversion coefficient $C_{23} = -C_u C_v \mp I_{32}$, for the \pm cases, we have, by Eq. (3.10) and the asymptotic behavior of Eqs. (3.11)–(3.21),

$$\begin{aligned} I_{32} &= \frac{1}{2\pi i \lambda^2} \int_{C_{\pm}} F_3(z) h(z) \Psi_2(z) dz , \\ &= \frac{1}{2\pi i \lambda^2} \int_{C_+} F_{vm}(y) h(y) \Psi_{up}(y) dy , \quad \text{for } + \text{ case} , \\ &= \frac{1}{2\pi i \lambda^2} \int_{C_-} F_{vp}(y) h(y) \Psi_{um}(y) dy , \quad \text{for } - \text{ case} , \end{aligned} \quad (3.26)$$

where $y = z - z_0$ and

$$\begin{aligned} \Psi_{up}(y) &\equiv T_u c_u \sum_{n=1}^{\infty} \frac{\alpha_{un}}{y^n} e^{i(y + \alpha_2 \ln y)} , \\ \Psi_{um}(y) &\equiv c_u^* \sum_{n=1}^{\infty} \frac{\alpha_{un}^*}{y^n} e^{-i(y + \alpha_2 \ln y)} , \\ F_{vp}(y) &\equiv T_v c_v \sum_{n=1}^{\infty} \frac{\tilde{\alpha}_{vn}}{y^n} e^{i(k_0 y + \alpha_4 \ln y)} , \\ F_{vm}(y) &\equiv c_v^* \sum_{n=1}^{\infty} \frac{\tilde{\alpha}_{vn}^*}{y^n} e^{-i(k_0 y + \alpha_4 \ln y)} , \end{aligned} \quad (3.27)$$

with c_u, c_v being the coefficients of u_+ and v_+ in Eqs. (3.5),

$$c_u = \frac{\pi \sqrt{T_u} \exp \{i[S(1) - s_u + z_0]\}}{C_u \alpha_1 (1 - k_0^2) \Gamma(i\alpha_2)} ,$$

$$c_v = \frac{\pi\sqrt{T_v} \exp\{i[S(k_0) - s_v + k_0 z_0]\}}{C_v \alpha_4 k_0 (1 - k_0^2) \Gamma(i\alpha_4)} .$$

Similarly, we can calculate the mode conversion coefficient $C_{32} = -C_u C_v \mp I_{23}$, with

$$\begin{aligned} I_{23} &= \frac{1}{2\pi i \lambda^2} \int_{C_{\pm}} F_2(z) h(z) \Psi_3(z) dz , \\ &= \frac{1}{2\pi i \lambda^2} \int_{C_+} F_{up}(y) h(y) \Psi_{vm}(y) dy , \quad \text{for + case ,} \\ &= \frac{1}{2\pi i \lambda^2} \int_{C_-} F_{um}(y) h(y) \Psi_{vp}(y) dy , \quad \text{for - case ,} \end{aligned} \quad (3.28)$$

where the definitions of F_{up} , F_{um} , Ψ_{vp} , and Ψ_{vm} are similar to Eqs. (3.27),

$$\begin{aligned} \Psi_{vp}(y) &\equiv T_v c_v \sum_{n=1}^{\infty} \frac{\alpha_{vn}}{y^n} e^{i(k_0 y + \alpha_4 \ln y)} , \\ \Psi_{vm}(y) &\equiv c_v^* \sum_{n=1}^{\infty} \frac{\alpha_{vn}^*}{y^n} e^{-i(k_0 y + \alpha_4 \ln y)} , \\ F_{up}(y) &\equiv T_u c_u \sum_{n=1}^{\infty} \frac{\tilde{\alpha}_{un}}{y^n} e^{i(y + \alpha_2 \ln y)} , \\ F_{um}(y) &\equiv c_u^* \sum_{n=1}^{\infty} \frac{\tilde{\alpha}_{un}^*}{y^n} e^{-i(y + \alpha_2 \ln y)} . \end{aligned} \quad (3.29)$$

From Eqs. (3.11)–(3.21), we also see that we can calculate the reflection coefficient $R_4 = C_v^2 \mp I_{44}$ by the series method, with

$$\begin{aligned} I_{44} &= \frac{1}{2\pi i \lambda^2} \int_{C_{\pm}} F_4(z) h(z) \Psi_4(z) dz , \\ &= \frac{1}{2\pi i \lambda^2} \int_{C_+} F_{vp}(y) h(y) \Psi_{vp}(y) dy , \quad \text{for + case ,} \\ &= \frac{1}{2\pi i \lambda^2} \int_{C_-} F_{vm}(y) h(y) \Psi_{vm}(y) dy , \quad \text{for - case .} \end{aligned} \quad (3.30)$$

However, we also see that the series method is not able to calculate the coefficients $R_2 = T_v^2 C_u^2 \pm I_{22}$ and $C_{24} = C_{42} = T_v C_u C_v \pm I_{42}$. The reason is that by Eqs. (3.11)–(3.21), $f_2 \propto v_p + u_p$ for $-\pi/2 < \theta < 0$ on C_+ and $f_2 \propto v_m + u_m$ for $\pi/2 < \theta < \pi$ on C_- . It is obvious that the contributions from the v_p or v_m terms to I_{22} or I_{42}

cannot be proved to be zero so that, e.g.

$$\begin{aligned} I_{22} &\neq \frac{1}{2\pi i \lambda^2} \int_{C_+} F_{up}(z) h(z) \Psi_{up}(z) dz , \\ I_{42} &\neq \frac{1}{2\pi i \lambda^2} \int_{C_+} F_{vp}(z) h(z) \Psi_{up}(z) dz , \end{aligned} \quad (3.31)$$

for the $+$ case. Moreover, we do not know how to calculate these contributions since v_p or v_m only appear on half of a semicircle. There is another reason that, as we will see, even if Eq. (3.31) were true, the series from the right hand sides are found to be divergent numerically.

To calculate the coefficients α_{un} and α_{vn} , we can substitute the asymptotic series of Ψ_{up} , and Ψ_{vp} of Eqs. (3.27) and (3.29), making use of Eq. (3.7), into Eq. (1.4), requiring that all terms vanish. The result for α_{un} is

$$\begin{aligned} \alpha_{un} &= a_{n,4} - (1 + k_0^2) a_{n,2} + k_0^2 a_{n,0} , \quad n \geq 1 , \\ a_{n,0} &= \frac{1}{2i\lambda^2(1 - k_0^2)n} \left\{ [\alpha_2 + i(n-1)] \left[\sum_{m=0}^5 a_{n-1,m} - \lambda^2 z_0 \alpha_{un} \right. \right. \\ &\quad \left. \left. - \lambda^2 (\alpha_2 + in) [a_{n-1,2} + 2a_{n-1,1} + (2 - k_0^2) a_{n-1,0}] \right. \right. \\ &\quad \left. \left. + \gamma_2 (a_{n-1,1} + a_{n-1,0}) \right] + \sum_{m=1}^{n-1} h_{n-m} \alpha_{um} \right\} , \\ a_{n,k} &= a_{n,k-1} + [\alpha_2 + i(n-1)] a_{n-1,k-1} , \quad k = 1, 2, 3, 4, 5, \end{aligned} \quad (3.32)$$

and $a_{0,k} = 1$. We can also use Eq. (3.32) to calculate $\tilde{\alpha}_{un}$ by putting $h_n = 0$.

Similarly for α_{vn} ,

$$\begin{aligned} \alpha_{vn} &= a_{n,4} - (1 + k_0^2) a_{n,2} + k_0^2 a_{n,0} , \quad n \geq 1 , \\ a_{n,0} &= \frac{1}{2i\lambda^2 k_0 (k_0^2 - 1) n} \left\{ [\alpha_4 + i(n-1)] \left[\sum_{m=0}^5 k_0^{5-m} a_{n-1,m} - \lambda^2 z_0 \alpha_{vn} \right. \right. \\ &\quad \left. \left. - \lambda^2 (\alpha_4 + in) [a_{n-1,2} + 2k_0 a_{n-1,1} + (2k_0^2 - 1) a_{n-1,0}] \right. \right. \\ &\quad \left. \left. + \gamma_2 (a_{n-1,1} + k_0 a_{n-1,0}) \right] + \sum_{m=1}^{n-1} h_{n-m} \alpha_{vm} \right\} , \end{aligned}$$

$$a_{n,k} = a_{n,k-1} + [\alpha_4 + i(n-1)] a_{n-1,k-1}, \quad k = 1, 2, 3, 4, 5, \quad (3.33)$$

and $a_{0,k} = 1$. Similarly we use Eq. (3.33) to calculate $\tilde{\alpha}_{vn}$ with $h_n = 0$.

Now that we have an exact asymptotic expansion of the integrands of Eqs. (3.26)–(3.30), we can write down the series expressions for those integrals, making use of the result

$$\begin{aligned} I_n^\pm &= \int_{C_\pm} \frac{dy}{y^n} e^{\pm i(\delta y + \Delta \ln y)} \\ &= 2\pi e^{\pi\Delta/2} \delta^{n-1 \mp i\Delta} (\pm i)^n / \Gamma(n \mp i\Delta), \end{aligned}$$

for real $\delta > 0$, where we have changed the contours of integration from C_\pm to C'_\pm in Figs. 2.1 and 2.2, using Hankel's contour integral Eq. (2.19).

We finally have, for the + case,

$$\begin{aligned} R_4 &= C_v^2 + \frac{i\pi^2 T_v^2 e^{2i[S(k_0) - s_v + k_0 z_0]}}{2\lambda^2 \alpha_4^2 k_0^3 (1 - k_0^2)^2 C_v^2 \Gamma^2(i\alpha_4)} (2k_0)^{2i\alpha_4} \sum_{n=3}^{\infty} \frac{\gamma_n (2ik_0)^n}{\Gamma(n + 2i\alpha_3)}, \\ C_{23} &= -C_u C_v - \frac{i\pi^2 T_u T_v e^{i[S(1) - S(k_0) - s_u + s_v + (1 - k_0)z_0]}}{\lambda^2 \alpha_2 \alpha_4 k_0 (1 - k_0^2)^2 C_u C_v \Gamma(i\alpha_2) \Gamma(i\alpha_3)} (1 - k_0)^{i(\alpha_1 - \alpha_3) - 1} \\ &\quad \times \sum_{n=3}^{\infty} \frac{\gamma_n [i(1 - k_0)]^n}{\Gamma[n + i(\alpha_1 - \alpha_3)]}, \end{aligned} \quad (3.34)$$

where γ_n is the coefficient of the y^{-n} terms of the integrand after combining the three series from F , Ψ , and h ,

$$\begin{aligned} \gamma_n &= \sum_{m=1}^{n-2} \beta_{n-m} h_m, \quad n \geq 3, \\ \beta_n &= \sum_{m=1}^{n-1} \alpha_{u(n-m)} \tilde{\alpha}_{vm}^*, \quad n \geq 2, \quad \text{for } C_{23}, \\ \beta_n &= \sum_{m=1}^{n-1} \alpha_{v(n-m)} \tilde{\alpha}_{vm}, \quad n \geq 2, \quad \text{for } R_4. \end{aligned} \quad (3.35)$$

The series for the – case is formally the complex conjugate of Eq. (3.34), but may have different h_n . The series for the coefficient C_{32} is also formally identical to the

C_{23} series in Eq. (3.34) with only a change of β_n in Eq. (3.35) to

$$\beta_n = \sum_{m=1}^{n-1} \tilde{\alpha}_{u(n-m)} \alpha_{vm}^* .$$

Note that we can also calculate the three corresponding coefficients for the eighth order equation (1.6) using Eq. (3.34) with the sign of the second term (the term with the summation) of both expressions changed to the opposite. But now, instead of Eq. (1.5),

$$\begin{aligned} \alpha_2 &= (1 - \gamma_6 + \gamma_2 - \gamma_0)/2\lambda^2(1 - k_0^2) , \\ \alpha_4 &= (-k_0^8 + \gamma_6 k_0^6 - \gamma_2 k_0^2 + \gamma_0)/2\lambda^2 k_0(1 - k_0^2) , \end{aligned}$$

and

$$S(k) = - \left\{ \frac{k^5}{5} + \frac{(1 + k_0^2 - \gamma_6)k^3}{3} + [(1 - \gamma_6)(1 + k_0^2) + k_0^4]k \right\} / \lambda^2 .$$

Also, $a_{n,0}$ in Eqs. (3.32) and (3.33) have to be calculated by slightly more complicated recurrence formulas respectively,

$$\begin{aligned} a_{n,0} &= \frac{1}{2i\lambda^2(1 - k_0^2)n} \left\{ [\alpha_2 + i(n-1)] \left[\sum_{m=0}^7 a_{n-1,m} - \gamma_6 \sum_{m=0}^5 a_{n-1,m} \right. \right. \\ &\quad \left. \left. - \lambda^2 z_0 \alpha_{un} - \lambda^2 (\alpha_2 + in) [a_{n-1,2} + 2a_{n-1,1} + (2 - k_0^2)a_{n-1,0}] \right. \right. \\ &\quad \left. \left. + \gamma_2 (a_{n-1,1} + a_{n-1,0}) \right] - \sum_{m=1}^{n-1} h_{n-m} \alpha_{um} \right\} , \\ a_{n,0} &= \frac{1}{2i\lambda^2 k_0 (k_0^2 - 1)n} \left\{ [\alpha_4 + i(n-1)] \left[\sum_{m=0}^7 k_0^{7-m} a_{n-1,m} - \gamma_6 \sum_{m=0}^5 k_0^{5-m} a_{n-1,m} \right. \right. \\ &\quad \left. \left. - \lambda^2 z_0 \alpha_{vn} - \lambda^2 (\alpha_4 + in) [a_{n-1,2} + 2k_0 a_{n-1,1} + (2k_0^2 - 1)a_{n-1,0}] \right. \right. \\ &\quad \left. \left. + \gamma_2 (a_{n-1,1} + k_0 a_{n-1,0}) \right] + \sum_{m=1}^{n-1} h_{n-m} \alpha_{vm} \right\} . \end{aligned}$$

Let us consider the nonrelativistic case using Eq. (3.23) as the h function first. The series for C_{23} in Eq. (3.34) is then evaluated numerically. Since the asymptotic

series of h for both \pm cases are the same, the C_{23} values from both cases are simply complex conjugate to each other so that the absolute values of them are identical. An empirical formula is found for it from numerical results,

$$|C_{23}|^2 \approx C_u^2 C_v^2 e^{-(1-k_0)^2 \kappa^2 / 2}, \quad (3.36)$$

for small $|\alpha_2|$, $|\alpha_4|$, not too small λ^2 and not too large κ . However, the series is not everywhere convergent. One radius of convergence is numerically found to be $k_0 > 1/3$ (Note again that k_0 has been chosen to be smaller than unity always), independent of other parameters. The analytical reason for this divergence is not clear for now, but it is found that this radius is not very clear cut. For not too small k_0 and not too large κ , the series first converges to a value expected by the empirical formula Eq. (3.36) and then diverges away. In Table 3.1 and 3.2, some values of $P_{23} \equiv 100|C_{23}|^2$ are shown, along with the values of q_{23} which is defined by $P_{23} = 100P_0 \exp[-q_{23}(1-k_0)^2 \kappa^2 / 2]$, with $P_0 \equiv C_u^2 C_v^2$. Note that q_{23} equals to unity if the empirical formula Eq. (3.36) gives the exact value. The values n in Table 3.1 is the number of terms summed in the evaluation of the series Eq. (3.34). For those values with $k_0 < 1/3$, we stop the evaluation at a term which has the smallest difference between the values if one more (or less) term is summed, because of the divergence problem. The n values for those data in Table 3.2 is from 150 to 153, but remain the same for each line of data. Note also that not all digits shown on these tables are significant figures. Only those digits without an underbar remain unchanged if one more (or less) term is summed. These non-convergent figures are shown in order to compare the convergence properties with other series.

One obvious quantity to be compared with C_{23} is the C_{32} coefficient, because mathematically it should be identical to C_{23} so that if the values from the series of

k_0	n	P_{32}	P_{23}	P'_{23}	q_{23}	q'_{23}
0.1	8	0.0618	0.0618	0.0627	1.0376	1.0280
0.2	8	0.0914	0.0914	0.0921	1.0067	1.0012
0.3	23	0.1258	0.1258	0.1262	0.9892	0.9860
0.4	157	0.1627	0.1627	0.1630	0.9890	0.9867
0.5	152	0.2023	0.2023	0.2025	0.9886	0.9870
0.6	147	0.2417	0.2417	0.2418	0.9882	0.9870
0.7	140	0.2776	0.2776	0.2777	0.9878	0.9868
0.8	132	0.3065	0.3065	0.3065	0.9873	0.9866
0.9	119	0.3252	0.3252	0.3252	0.9867	0.9863
0.95	109	0.3300	0.3300	0.3300	0.9863	0.9861
0.99	90	0.3316	0.3316	0.3316	0.9860	0.9860
0.999	72	0.3317	0.3317	0.3317	0.9860	0.9860

Table 3.1: Nonrelativistic case with $\lambda^2 = 20$, $|\alpha_2| = 0.12$, $|\alpha_4| = 0.001$ and $\kappa = 2$. Note that $P_0 = 0.3317\%$.

κ	P_{32}	P_{23}	P'_{23}	q_{32}	q_{23}	q'_{23}
0.1	0.3312	0.3312	0.3312	0.9904	0.9904	0.9903
0.5	0.3216	0.3216	0.3216	0.9903	0.9903	0.9902
1	0.2930	0.2930	0.2931	0.9902	0.9902	0.9900
2	0.2022	0.2022	0.2022	0.9894	0.9894	0.9892
4	4.622e-2	4.622e-2	4.625e-2	0.9853	0.9853	0.9851
6	4.148e-3	4.148e-3	4.157e-3	0.9737	0.9736	0.9732
8	1.801e-4	1.803e-4	1.818e-4	0.9398	0.9397	0.9386
10	6.603e-6	6.694e-6	6.830e-6	0.8660	0.8649	0.8632
12	2.560e-7	2.843e-7	2.918e-7	0.7819	0.7761	0.7746
14	7.887e-9	1.522e-8	1.556e-8	0.7165	0.6897	0.6888
16	1.916e-10	3.434e-9	3.454e-9	0.6647	0.5746	0.5744
18	4.419e-12	3.787e-9	3.787e-9	0.6183	0.4516	0.4516
20	2.831e-11	6.346e-9	6.248e-9	0.4637	0.3554	0.3557
22	345.3	345.3	345.3	-0.1148	-0.1148	-0.1148

Table 3.2: Nonrelativistic case with $\lambda^2 = 200$, $|\alpha_2| = 0.12$, $|\alpha_4| = 0.001$ and $k_0 = 0.5$. Note that $P_0 = 0.3317\%$.

these two differ with each other, we know they cannot be both correct. This may indicate that both values are not truly converged or there are other errors. So we also show the values of $P_{32} \equiv 100|C_{32}|^2$ in Table 3.1 and 3.2. The values of q_{32} defined similarly as q_{23} are also shown in Table 3.2. We see that the two quantities P_{23} and P_{32} are identical to each other when $k_0 \geq 0.3$ and $\kappa < 10$. The deviation for small k_0 is obviously due to the divergence problem of the series. Also, when κ starts to grow larger, we know from calculations that the terms in the series grow to large values and then decrease, but at the same time the coefficient tends to zero. Since we can only compute it using finite precision and only a finite number of terms can be summed, we expect that the series will effectively diverge after some large κ value. The fact that P_{23} and P_{32} in Table 3.2 do not get smaller for $\kappa > 18$ shows the error is starting to get large so that the values before that are also not converged to the true values due to the subtraction errors. This can be seen by the fact that $P_{23} \neq P_{32}$ for $12 < \kappa$. One interesting fact is that P_{23} agrees with P_{32} again after the series obviously has encountered numerical difficulties (see the values at $\kappa = 22$). Different from the divergence problem for small k_0 , this error is only numerical and there does not exist a clear cut radius of convergence of κ .

Another quantity to compare with is the C_{23} coefficient from the eighth order equation (1.6). The values of P'_{23} and q'_{23} , defined similarly, are also shown in Table 3.1 and 3.2. We see that the values of P'_{23} , q'_{23} are very close to P_{23} and q_{23} respectively, even for those values that are not truly converged. This shows that the two series have very similar convergence properties. This agreement is also found to be true for cases with different parameters. Obviously, the empirical formula Eq. (3.36) is also valid for this case.

An empirical formula is also found for R_4 ,

$$|R_4|^2 \approx C_v^4 e^{-2k_0^2 \kappa^2} ,$$

for small $|\alpha_2|$, $|\alpha_4|$, not too small λ^2 and not too large κ . This empirical formula is consistent with that for R_2 of the fourth order equation (1.2), $|R_2|^2 \approx C^4 \exp(-2\kappa^2)$, since as $|\alpha_2| \rightarrow 0$, the five branch problem represented by Eq. (1.4) becomes a three branch problem represented by Eq. (1.2) and then $R_4 \rightarrow R_2$ with $k_0 \kappa \rightarrow \kappa$. However, the radius of convergence for this series is $k_0 < 1/3$, just opposite to that of the series of C_{23} . For k_0 larger and near $1/3$, the series also first apparently converges to a certain reasonable value and then diverges away.

Let us now consider the relativistic case by using Eqs. (3.24) as the h function. Since now the h function for the \pm cases are slightly different, we will do our calculation mainly on the $-$ case. The empirical formula for C_{32} is now

$$|C_{23}|^2 \approx C_u^2 C_v^2 e^{-7(1-k_0)^2 \kappa^2 / 2} . \quad (3.37)$$

The radius of convergence $k_0 > 1/3$ is still true for this case, but now there is another radius of convergence $(1 - k_0)\kappa < 1$, similar to the radius of convergence $\kappa < 0.5$ for R_2 from Eq. (1.2) for the relativistic case. Some values of P_{23} , and q_{23} , which is now defined by $P_{23} = 100P_0 \exp[-q_{23} 7(1 - k_0)^2 \kappa^2 / 2]$, are shown in Table 3.3 and 3.4. Note that this empirical formula Eq. (3.37) also works for the $+$ case. Actually, it works even slightly better than the $-$ case. The values of C_{23} are generally close for the two cases. The q_{23} values for the $+$ case, which we call q_{23}^+ , are also shown in Table 3.3.

We also did calculations on C_{32} for both cases. The values of C_{23} and C_{32} agree if the series is convergent. We did not show C_{32} and q_{32} in Table 3.3 and 3.4 because

k_0	n	P_{23}	P'_{23}	q_{23}	q'_{23}	q_{23}^+
0.1	8	0.1313	0.0985	0.9082	0.9249	0.9922
0.2	15	0.1657	0.1364	0.8606	0.8573	0.9253
0.3	31	0.1923	0.1649	0.8824	0.8799	0.9447
0.35	159	0.2062	0.1803	0.8929	0.8907	0.9532
0.4	157	0.2202	0.1961	0.9030	0.9012	0.9610
0.5	152	0.2480	0.2284	0.9222	0.9210	0.9744
0.6	146	0.2744	0.2600	0.9397	0.9389	0.9845
0.7	140	0.2976	0.2886	0.9551	0.9546	0.9909
0.8	131	0.3159	0.3115	0.9681	0.9679	0.9934
0.9	119	0.3276	0.3264	0.9785	0.9784	0.9918
0.95	108	0.3306	0.3303	0.9826	0.9825	0.9894
0.99	90	0.3316	0.3316	0.9853	0.9853	0.9867
0.999	72	0.3317	0.3317	0.9859	0.9859	0.9860

Table 3.3: Relativistic case with $\lambda^2 = 100$, $|\alpha_2| = 0.12$, $|\alpha_4| = 0.001$ and $\kappa = 0.6$. Note that $P_0 = 0.3317\%$.

κ	P_{23}	P''_{23}	P'_{23}	q_{23}	q''_{23}	q'_{23}
0.6	0.3276	0.3276	0.3264	0.9785	0.9784	0.9784
0.8	0.3245	0.3245	0.3225	0.9749	0.9748	0.9747
1.0	0.3206	0.3206	0.3175	0.9709	0.9708	0.9707
1.2	0.3159	0.3159	0.3115	0.9666	0.9664	0.9664
1.35	0.3119	0.3119	0.3065	0.9631	0.9629	0.9628
1.5	0.3075	0.3075	0.3010	0.9594	0.9592	0.9591
1.6	0.3044	0.3044	0.2971	0.9568	0.9567	0.9565
1.8	0.2977	0.2977	0.2887	0.9514	0.9512	0.9511
2.0	0.2905	0.2905	0.2798	0.9457	0.9455	0.9453
2.2	0.2829	0.2829	0.2703	0.9396	0.9394	0.9391
2.5	0.2706	0.2706	0.2554	0.9300	0.9298	0.9294
3.0	0.2488	0.2488	0.2293	0.9125	0.9123	0.9117
3.5	0.2261	0.2261	0.2028	0.8935	0.8933	0.8924
4.5	0.1813	0.1814	0.1528	0.8520	0.8517	0.8501
6.0	0.1234	0.1234	0.0935	0.7846	0.7844	0.7816
8.0	0.06999	0.07004	0.0454	0.6945	0.6942	0.6903

Table 3.4: Relativistic case with $\lambda^2 = 100$, $|\alpha_2| = 0.12$, $|\alpha_4| = 0.001$, $k_0 = 0.9$ and $n = 119$. Note that $P_0 = 0.3317\%$.

they are simply the same as C_{23} and q_{23} . The empirical formula of R_4 for this case is,

$$|R_4|^2 \approx C_v^4 e^{-14k_0^2 \kappa^2},$$

for small $|\alpha_2|$, $|\alpha_4|$, not too small λ^2 and not too large κ . This empirical formula is also consistent with that for R_2 from Eq. (1.2), $|R_2|^2 \approx C^4 \exp(-14\kappa^2)$.

The values of P'_{23} and q'_{23} calculated by using Eq. (3.25) as the h function for the eighth order equation (1.6), are also shown in Tables 3.3 and 3.4. Because of the difference in the h function, the empirical formula for this case becomes

$$|C_{23}|^2 \approx C_u^2 C_v^2 e^{-9(1-k_0)^2 \kappa^2/2}. \quad (3.38)$$

As a result, the P'_{23} values in Tables 3.3 and 3.4 are generally different from the P_{23} values, but still q'_{23} are very close to q_{23} , where q'_{23} is now defined by $P'_{23} = 100P_0 \exp[-q'_{23}9(1-k_0)^2 \kappa^2/2]$. If we use the negative of Eq. (3.24) as the h function instead, and calculate P''_{23} and q''_{23} defined similarly to P_{23} and q_{23} , even the values of P''_{23} will be very close to those of P_{23} as can be seen from Table 3.4. This shows that the convergence properties of the two series from the sixth and eighth order equations are very similar. Similarly, the empirical formula of R_4 for this case is,

$$|R_4|^2 \approx C_v^4 e^{-18k_0^2 \kappa^2},$$

We see that the factor before κ^2 in these empirical formulas depend on the h function rather than the order of the equation, namely the factors are 7 and 14 if we use $F_{7/2}$ or 9 and 18 when we use $F_{9/2}$.

The fact that the C_{23} series diverges for $k_0 < 1/3$ and the R_4 series diverges for $k_0 > 1/3$ makes it very difficult to get both values for the same k_0 accurately,

except for k_0 near $1/3$. Although we do not understand this divergence analytically, we may try to see how the $k_0 = 1/3$ limit comes about by looking at the two series in Eq. (3.34). Note that the n th term of the series of C_{23} is proportional to $(1 - k_0)^n$ and that of R_4 is proportional to $(2k_0)^n$. These two factors $1 - k_0$, and $2k_0$ are equal when $k_0 = 1/3$. From this we can also see another reason why we cannot calculate R_2 and C_{24} by the series method. In order to calculate them, we must evaluate the series from the right hand side of Eq. (2.15). It is obvious that the n th term of these two series is proportional to 2 and $1 + k_0$ respectively, which are larger than $2/3$ for all k_0 . So these two series should be seriously divergent. Indeed we found that it is so numerically. Therefore, it seems that we cannot calculate R_2 and C_{24} by the series method, at least in the present formulation.

From these empirical formulas (3.36) to (3.38) of C_{23} and other numerical results, we see that although C_{23} is not exactly independent of absorption, the dependence is much weaker than other coefficients because of the $(1 - k_0)^2/4$ factor, if k_0 is close to unity. Note that the empirical formula for R_2 should be proportional to $\exp(-2\kappa^2)$, for the nonrelativistic case, similar to that of Eq. (1.2), but C_{23} is only proportional to $\exp[-(1 - k_0)^2\kappa^2/2]$. Note also that the factor $C_u^2 C_v^2$ is usually very small for a plasma, since the O-mode transmission coefficient is usually very close to unity so that one of the factors C_u or C_v is very small, depending on which one represents the O-mode. Therefore, when calculating the coefficient C_{23} from solving the integral equation numerically, usually only one or two significant figures can be obtained for realistic cases. Due to the weak dependence on absorption, these one or two significant figures remain unchanged even after other scattering parameters have decayed to relatively small values. Another factor is that the numerical method

that solves the integral equation also does not converge for large κ . So, it is hard to see how C_{23} changes for really large absorption using that method. That explains why the previous result indicated that C_{23} is independent of absorption [36, 34], since the k_0 values used there were all close to unity.

Discussion

Although subject to some divergence problems, the series method once again shows its power in calculating fast wave scattering parameters. We now know that it works for equations with order higher than four and for five branch problems as well as three branch problems. It can be used to calculate C_{23} , for situations with even stronger absorption, with much higher accuracy and efficiency than solving the integral equations numerically. This enables us to conclude definitely that it does depend on absorption and we can even find empirical formulas for it for different absorption functions. From these results, we know that the dependence on absorption is usually weak so that we can explain why this dependence was not found by the previous study.

The dependence of C_{23} on absorption indeed satisfies the separation scheme for very strong absorption. Since the mode conversion coefficients of the two separated three branch problems all vanish for very strong absorption, the conversion coefficient C_{23} between the two must also vanish. However, because of the weak dependence on absorption of C_{23} , it may not change much for moderately strong absorption, even when the mode conversion coefficients of the two separated problems all become very small. This means that the separation scheme still does not work very well here, not until the absorption becomes extremely strong. This is a

fact that should be taken into consideration by any theory that treats the five branch problem as two separated three branch problems. This also shows that solving these higher order equations for the five branch problem may provide more advantages than the separation scheme, even for moderately strong absorption. One example here is that the weak dependence of C_{23} , found by solving these higher order equations, will be difficult to imagine using the separation scheme.

ANALYTIC CALCULATIONS OF CERTAIN
SCATTERING PARAMETERS FROM MODE
CONVERSION EQUATIONS

CHAPTER 4

IV. CONCLUSION

Let us summarize our contribution to the calculations of scattering parameters from mode conversion equations. First, we have extended the proof showing that some fast wave scattering parameters are independent of absorption for a fourth order three branch problem to a sixth order five branch problem. Because of this, we should be more confident that similar proofs may also exist for even higher order equations. Second, we have developed an analytical method that can find the series expressions for some scattering parameters, for both three and five branch problems. We have checked the correctness of this method by comparing its results to that by solving the integral equation iteratively for the fourth order three branch problem. Also, we have checked the consistency of the method by showing that the results from the series method satisfy the proved reciprocity relation for the five branch problem. From the numerical results from the series method, many empirical formulas for those scattering parameters have been found. Thus, it is concluded that the mode conversion coefficient C_{23} of a five branch problem is not exactly independent of absorption, but usually has weak dependency. This enables us to explain a previous numerical result which was unexpected because of its contradiction with the separation treatment of a five branch problem as two three branch problems. We also showed that the results from equations that represent physical situations of second cyclotron harmonics are very similar to those from equations that represent third harmonics, for both three and five branch problems.

The advantages of the series method are several. First, it is an analytical method in nature, although the series is quite complicated, so that it enables further analytical studies and development. Secondly, it is a quite efficient method in computation because we do not need to find the solutions for the equation itself, which are required by the method that solves the integral equation numerically. Third, it is usually more accurate, when the divergent problem is not very serious, and we may try to increase the accuracy by summing more terms or increasing the precision of the real numbers of the computations.

There are two problems with the series method. First, it is not always convergent for all absorption functions h or for all parameter ranges. Moreover, the convergence properties of this method are difficult to investigate because of its complicated nature. Thus, there is no good criterion to tell when does the series converges for now. Secondly, it does not work for all scattering parameters. The series for the slow wave scattering parameters are seriously divergent, as are some fast wave scattering parameters for the five branch problem.

As pointed out in the introduction, the mode conversion effects have been used for heating or diagnosis of plasmas, so the method we developed here may help in these applications. For some situations where the model equations can represent the physics relatively well, the scattering parameters calculated by this method can be used directly to interpret or to predict experimental results. For more complicated situations which have to be solved numerically by more sophisticated computer programs, our method may provide some limiting situations so that the validity of these programs can be checked efficiently. Some numerical methods, e.g., ray tracing, cannot treat the situations near the mode conversion point and thus a

separated subroutine has to be used to solve the mode conversion problem there in order to get a continuous solution. Our method may be used to improve the efficiency and accuracy in such subroutines.

Since our results confirmed that the coupling between the X-mode and the O-mode may be much stronger than we used to believe for strong absorption cases, this fact has to be taken into account for any theory involving the X-mode – O-mode coupling. Some applications using the X-mode – O-mode coupling, e.g., to transmit wave energy to a region where only one mode exists from a region where this mode does not exist, may be more efficient than expected.

In conclusion, the development of the series method significantly increases our understanding of the mode conversion equations. Some results, which are difficult to find by numerical methods, have been found by applying the series method. There are still many difficult problems with the series method to be considered by further research.

ANALYTIC CALCULATION OF CERTAIN SCATTERING
PARAMETERS FROM MODE CONVERSION
EQUATIONS

BIBLIOGRAPHY

BIBLIOGRAPHY

- [1] N. S. Erokhin, Ukr. Fiz. Zh. **14**, 2055 (1969) (English translation not available);
N. S. Erokhin and S. S. Moiseev, *Reviews of Plasma Physics*, (Consultants
Bureau, New York, 1979), Vol. 7, p. 181.
- [2] Y. C. Ngan and D. G. Swanson, Phys. Fluids **20**, 1920 (1977).
- [3] T. H. Stix and D. G. Swanson, *Handbook of Plasma Physics* edited by
A. A. Galeev and R. N. Sudan, (North-Holland Publishing Co., 1983), Vol. 1,
p.335.
- [4] D. G. Swanson, *Plasma Waves*, (Academic Press, Boston, 1989).
- [5] D. G. Swanson, Nucl. Fusion **20** 428 (1980).
- [6] P. L. Colestock and R. J. Kashuba, Nucl. Fusion **23**, 763 (1983).
- [7] D. G. Swanson, Phys. Fluids **28**, 2645 (1985).
- [8] T. H. Stix, Phys. Rev. Lett. **15**, 878 (1965).
- [9] F. Engelmann and M. Curatolo, Nucl. Fusion **13**, 497 (1973).
- [10] S. M. Wolfe, D. R. Cohn, R. J. Temkin, and K. Kreischer, Nucl. Fusion **19**, 389
(1979).
- [11] B. Hui, K. R. Chu, E. Ott, and T. Antonsen, Phys. Fluids **23**, 822 (1980).

- [12] A. E. Costly, R. J. Hastie, J. W. M. Paul, and J. Chamberlain, *Phys. Rev. Lett.* **33**, 758 (1974).
- [13] I. H. Hutchinson and D. S. Komm, *Nucl. Fusion* **17**, 1077 (1977).
- [14] W. R. Rutgers and D. A. Boyd, *Phys. Lett.* **39**, 408 (1977).
- [15] O. Eldridge, W. Namkung, and A. C. England, Report ORNL/TM-6052 (1978).
- [16] V. Arunasalam, E. B. Meservey, M. N. Gurnee, and R. C. Davidson, *Phys. Fluids* **11**, 1076 (1968).
- [17] K. G. Budden, *Radio Waves in the Ionosphere*, Cambridge 1961.
- [18] W. Wasow, *Ann. Math.* **52**, 350 (1950).
- [19] A. L. Rabenstein, *Arch. Ration. Mech. Anal.* **1**, 414 (1958).
- [20] T. H. Stix, *Phys. Fluids* **3**, 19 (1960).
- [21] V. E. Golant and A. D. Piliya, *Sov. Phys. Usp.* **14**, 413 (1972).
- [22] D. W. Faulconer, *Phys. Lett.* **75A**, 355 (1980).
- [23] T. M. Antonsen, Jr. and W. M. Manheimer, *Phys. Fluids* **21** 2295 (1978).
- [24] D. G. Swanson and V. F. Shvets, *J. Math. Phys.* **34**, 69 (1993).
- [25] C. S. Ng and D. G. Swanson, *Phys. Plasma* **1** 815 (1994).
- [26] T. Hellsten, K. Appert, J. Vaclavik, and L. Villard, *Nucl. Fusion* **25**, 99 (1985).
- [27] E. F. Jaeger, D. B. Batchelor, and H. Weitzner, *Nucl. Fusion* **28**, 53 (1988).

- [28] Huanchun Ye and Allan N. Kaufman, *Phys. Rev. Lett.* **61**, 2762 (1988).
- [29] A. Kay, R. A. Cairns, and C. N. Lashmore-Davies, *Plasma Phys. Controlled Fusion* **30**, 471 (1988).
- [30] C. N. Lashmore-Davies, V. Fuchs, G. Francis, A. K. Ram, A. Bers, and L. Gauthier, *Phys. Fluids* **31**, 1614 (1988).
- [31] V. Fuchs and A. Bers, *Phys. Fluids* **31**, 3702 (1988).
- [32] C. Chow, V. Fuchs, and A. Bers, *Phys Fluids B* **2**, 2185 (1990).
- [33] D. G. Swanson, *Phys. Fluids* **28**, 1800 (1985).
- [34] Jianlong Hu, Ph.D. Dissertation, Auburn University, Auburn, Alabama, 1993.
- [35] J. L. Hu and D. G. Swanson, *Phys. Fluids B* **5**, 4207 (1993).
- [36] J. L. Hu and D. G. Swanson, *Phys. Fluids B* **5**, 4221 (1993).
- [37] D. J. D. Gambier and J. P. M. Schmitt, *Phys. Fluids* **26**, 2200 (1983).
- [38] D. J. Gambier and D. G. Swanson, *Phys. Fluids* **28**, 145 (1985).
- [39] Suwon Cho and D. G. Swanson, *Phys. Fluids B* **2** 2704 (1990).
- [40] M. Abramowitz and I. Stegun, *Handbook of Mathematical Functions* (National Bureau of Standards, Washington, D.C., 1964).
- [41] I. P. Shkarofsky, *Phys. Fluids* **9**, 561 (1966).
- [42] P. A. Robinson, *J. Math. Phys.* **30**, 2484 (1989).

- [43] V. I. Krylov and N. S. Skoblya, *A Handbook of Methods of Approximate Fourier Transformation and Inversion of the Laplace Transformation*, (Mir Publishers, Moscow, 1977).

ANALYTIC CALCULATIONS OF CERTAIN
SCATTERING PARAMETERS FROM MODE
CONVERSION EQUATIONS

APPENDIX

Appendix: A Simple Example

To give a simple example of the integration method that generates those series expressions in the main text, we use it to calculate the Fourier transform of the plasma dispersion function $Z(x)$ for real x . Note that this is actually a rather established method to calculate Fourier or Laplace transforms[43]. Let us calculate

$$\tilde{Z}(k) \equiv \int_{-\infty}^{\infty} Z(x)e^{ikx} dx ,$$

for real k . Now $Z(x)$ is analytic in the upper x -plane, so we can change the integration contour to the C_- contour defined in Fig. 2.2. Note that on C_- , we can expand $Z(x)$ as an asymptotic series similar to that in Eq. (2.11). Then

$$\tilde{Z}(k) \equiv - \int_{C_-} \sum_{n=0}^{\infty} \frac{\Gamma(n + 1/2)e^{ikx}}{\Gamma(1/2)x^{2n+1}} dx .$$

If $k > 0$, then $Z(k) = 0$ obviously. For $k < 0$, we can close the contour C_- with another semicircle on the lower x -plane without adding any contribution. The integration contour then becomes a circle with infinite radius going clockwise around the origin. So we can now evaluate the above integral using the Residue Theorem, since there is a pole at $x = 0$. Using

$$\text{Res} \left\{ \frac{e^{ikx}}{x^{2n+1}} \right\} = \frac{1}{(2n)!} \frac{d^{2n}}{dx^{2n}} (e^{ikx})_{x=0} = \frac{(-k)^{2n}}{(2n)!} ,$$

we finally have

$$\tilde{Z}(k) = 2\pi i \sum_{n=0}^{\infty} \frac{1}{n!} \left(\frac{-k^2}{4} \right)^n \Theta(-k) = 2\pi i e^{-k^2/4} \Theta(-k),$$

where $\Theta(x)$ is the step function which equals to 1 for $x > 0$, and equals to 0 for $x < 0$. In order to check whether this result is correct, we calculate the inverse Fourier transform of it, which should be equal to $Z(x)$, i.e. we want to check whether

$$Z(x) = \frac{1}{2\pi} \int_{-\infty}^{\infty} \tilde{Z}(k) e^{-ikx} dk = i \int_0^{\infty} e^{ikx - k^2/4} dk.$$

By Expanding the $\exp(ikx)$ factor as

$$e^{ikx} = \sum_{n=0}^{\infty} \frac{(ikx)^n}{n!}$$

and using

$$\begin{aligned} \int_0^{\infty} k^{2n+1} e^{-k^2/4} dk &= 2^{2n+1} n!, \\ \int_0^{\infty} k^{2n} e^{-k^2/4} dk &= 2^n (2n-1)!! \sqrt{\pi}, \end{aligned}$$

we finally have

$$\begin{aligned} Z(x) &= i\sqrt{\pi} e^{-x^2} - 2x \left[1 - \frac{2x^2}{3} + \frac{4x^4}{3 \cdot 5} - \dots + \frac{(-2x^2)^n}{(2n+1)!!} \right] \\ &= i\sqrt{\pi} \sum_{n=0}^{\infty} \frac{(ix)^n}{\Gamma(\frac{n}{2} + 1)}, \end{aligned}$$

which is simply the power series expansion of $Z(x)$ [4]. This means that the Fourier transform calculated by our integration method is indeed correct. It is also interesting to note that we start from using the asymptotic expansion of $Z(x)$ to calculate its Fourier transform, but we get its series expansion instead after we perform the inverse Fourier transform. This provides a relation between the two series.